CROSS-LINKING OF SATURATED LONG-CHAIN HYDROCARBONS

by

Kogilambal Ishripersadh

SUBMITTED IN FULFILMENT OF THE REQUIREMENTS FOR THE DEGREE

MASTERS OF TECHNOLOGY : CHEMISTRY

IN THE DEPARTMENT OF CHEMISTRY

IN THE FACULTY OF SCIENCE

AT THE ML SULTAN TECHNIKON

DATE SUBMITTED : FEBRUARY 1999

SUPERVISOR : PROF AS LUYT, UNIVERSITY OF THE NORTH (QWA-QWA)

CO-SUPERVISOR : MS DN TIMM

DECLARATION

I declare this dissertation is my own, unaided work. It is submitted for the degree of Masters of Technology: Chemistry in the Department of Chemistry in the Faculty of Science at the M L Sultan Technikon in Durban.

26 February 1999

Kogilambal Ishripersadh

CONTENTS

ACKNOWLEDGEMENTS

The author would like to express special thanks to Mr B Bisnath (Head of the Department : Chemistry, ML Sultan Technikon) and Prof KG Moodley (Associate Research Director : Chemistry, ML Sultan Technikon) for their assistance, willing support and guidance. In addition I would like to thank the Department of Chemistry, especially Ms V Moonsamy and Mr K Bisetty, for all the moral support and input.

The Technikon is acknowledged for its financial assistance.

A special thanks to Ms L Spencer (Laboratory Manager), Ms B Blair (Chemist) and Ms Ishana Singh of Dunlop, BTR for the assistance in the use of their FTIR.

I would also like to thank my husband Roy and daughter Dhirasha for their support and tolerance throughout my studies.

Lastly, but above all I wish to express my eternal gratitude to my supervisor, Prof AS Luyt (Director of Research, University of the North (Qwa-Qwa)), and co-supervisor, Ms DN Timm, for their enduring support, encouragement, patience and guidance.

ABSTRACT

Saturated long chain hydrocarbons, such as paraffin waxes, have a large variety of applications. These applications may, however, be restricted by certain properties of the wax such as brittleness and in compounding. Cross-linking of the long chains in waxes may provide improved physical properties and hence a wider application of these waxes.

Chemical cross-linking involves initiation by relatively stable peroxides, such as dicumyl peroxide (DCP). The peroxides are stable at normal processing temperatures, but decompose to provide free radicals for cross-linking at higher temperatures in a post-processing vulcanization or curing reaction.

In this study, dicumyl peroxide and potassium persulphate were used as curing agents in a comparative study of the cross-linking of three types of petroleum waxes. Thermal analysis techniques, Fourier-transform infra-red, photoacoustic Fourier-transform infra-red and gel content was used to determine the extent of cross-linking.

It was found that dicumyl peroxide effectively cross-links all the investigated waxes, and that the extent of cross-linking is proportional to the DCP/wax m/m ratio. Potassium persulphate (PPS), however, did not initiate cross-linking in any of the wax samples, despite a strong DSC exotherm in the same temperature range than the cross-linking exotherm observed when DCP was used as cross-linking agent.

CHAPTER ONE

INTRODUCTION

Petroleum waxes have a variety of applications in the polish, paint, ink and candle molding industries. However, a certain type of wax may, for example, only be used for polishes and not paints. The modification through cross-linking of three different types of petroleum waxes was investigated.

1.1 Saturated long-chain hydrocarbons

Petroleum and natural gas are substances that consist almost entirely of a complete mixture of molecular compounds called hydrocarbons [1]. Hydrocarbons are made from the atoms of just two elements, carbon and hydrogen, and if the covalent bond between the carbon atoms is single, it is described as a *saturated hydrocarbon* as indicated in Figure 1.1.

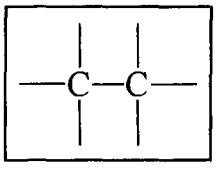

Figure 1.1 A saturated hydrocarbon

If the carbon skeleton in a long hydrocarbon chain has no additional carbon atoms attached to it at intermediate points, that is in the absence of carbon branches, the carbon skeleton may be referred to as a straight chain. The difference between hydrocarbon gases, liquids and solids (waxes and polymers) lies in their molecular structure [2]. The physical properties of the hydrocarbon change as the chain length increases:

C_1 - C_4	exist as gases at ambient temperature
C_5 - C_{12}	exist as volatile liquids
C_{13} - C_{18}	exist as higher boiling liquids
$>C_{19}$	exist as heavy oils and waxes

1.2 Waxes

The German Society for Wax (Fat) Science formulated the following definition for a wax [3]:

'Wax is a collective technological term for a series of natural and synthetic substances that, as a rule, have the following properties : can be a solid, pliable to hard, brittle at 20 °C, coarse or fine crystalline, translucent or opaque but not glassy, melt above 40 °C without decomposition, having a relatively low viscosity just above its melting point, cannot be drawn into threads, consistency and solubility strongly dependent upon temperature and can be polished under slight pressure'

Waxes occur naturally as animal, vegetable and mineral wax or may be synthesized [4].

1.2.1 Animal waxes

Animal waxes include beeswax, spermaceti, wool grease and lanolin. A considerable quantity of beeswax is used in candle making and molding.

1.2.2 Vegetable waxes

The vegetable waxes include carnauba, ouricoun (palm wax) and candilla. These three waxes constitute the major proportion of the consumption of vegetable waxes. Jojoba oil is said to be a newcomer and it is the only available wax produced from plantation grown plants.

1.2.3 Mineral waxes

This category of waxes includes ozokerite, montan and petroleum or paraffin waxes [4].

i) Ozokerite

Ozokerite is a black solid, the hardness of which varies with its source and degree of refining. It is a 'tacky' wax which sets more rapidly and with more shrinkage than beeswax. It has a microcystalline structure and tends to be less soluble in organic solvents than paraffin wax. Ozokerite is used in lubricants, lipsticks, deodorants, adhesives and polishes.

ii) Montan wax

Montan wax is a very hard wax and is one of the waxes most resistant to oxidation. Single-use carbon papers is the largest consumer of crude montan wax.

iii) Microcrystalline waxes

Microcrystalline waxes may be obtained as by-products from de-waxing lube oil or de-oiling of settlings obtained from crude oil held in storage. The high viscosity distillates can yield microcrystalline waxes after they have been diluted with solvents and cooled. The wax can be separated by centrifugation. The most widely used de-waxing solvent is methyl ethyl ketone. Microcrystalline waxes give less lustre but are tougher and more flexible than common paraffin waxes. They are used in flexible packaging and in hot-melt adhesives.

iv) Paraffin / petroleum wax

Paraffin waxes may be produced in one of the following processes [4] :

* De-waxing of petroleum products
* De-oiling and fractional crystallization of petroleum waxes
* Purification of crude paraffin waxes.
* Blending of paraffin waxes with additives

The waxes of crude petroleum oils are obtained by distillation followed by a chilling process, when the resultant slurry is passed through a filter press. The wax left is called slack wax. The wet filter cake is then treated with acid and the sludge withdrawn, neutralized and washed. The slack wax is melted, poured into trays, held in a sweating oven and allowed to cool. The temperature is gradually raised until an oil or soft wax 'sweats' out. After a further distillation black wax is produced which is treated with sulphuric acid to remove most of the colour. Final bleaching is then done to give a fully refined paraffin wax. Paraffin waxes are used to promote water resistance. They are used in certain packaging applications and candles.

1. 3 Cross-linking

Cross-linking may be described [5] as the attachment of two chains of polymer molecules by bridges of either an element, a group or a compound which joins certain carbon atoms of the chain by a primary chemical bond as illustrated in Figure 1. 2.

Typical starting materials [1] e.g.

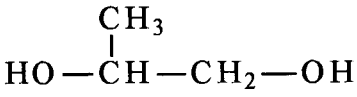

propylene glycol

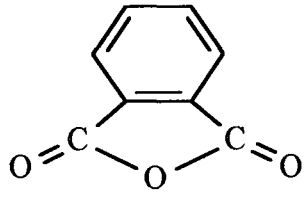

phthalic anhydride

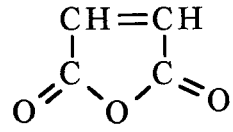

maleic anhydride

Starting materials represented by the following symbols :

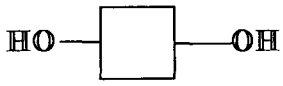

propylene glycol

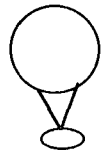

phthalic anhydride

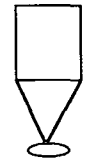

maleic anhydride

Polymerization → linear unsaturated polyester

↓

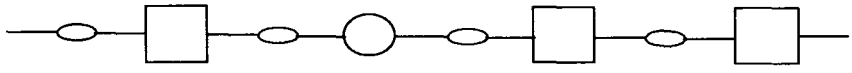

The addition of a vinyl monomer e.g. (Δ) is cross-linked by free radical initiator

↓

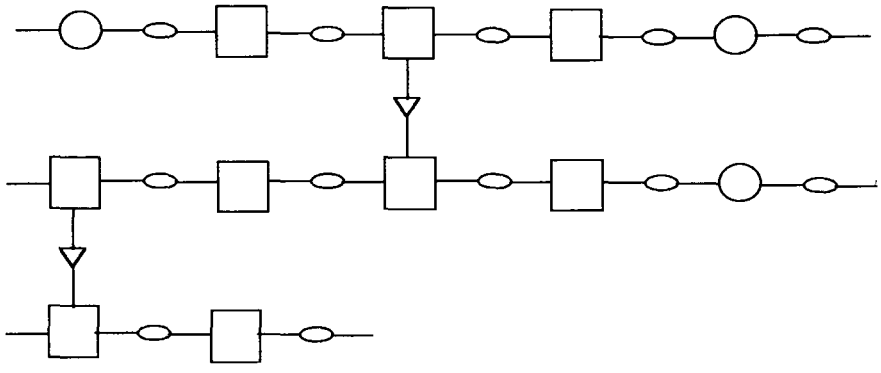

Figure 1.2 Schematic representation of cross-linked polyester

Cross-linking can be effected artificially, either by addition of a chemical substance (cross-linking agent) and exposing the mixture to heat, or by subjecting the polymer to high energy radiation. The introduction of cross-links has the effect of changing a plastic from thermoplastic, i.e. its ability to soften and take on new shapes by application of heat and pressure, to a final product which is stable to heat, and which cannot flow or melt (thermoset)[6]. In commercial practice, cross-linking reactions may take place during the fabrication of items made with thermosetting resins. The addition of cross-links leads to increased strength, heat and electrical resistance and especially resistance to solvents.

1.3.1 Chemical cross-linking

Chemical cross-linking [6] is achieved by incorporation of relatively stable peroxides, such as di-cumyl peroxide and di-t-butyl peroxide. These stable peroxides are known as cross-linking/curing agents and provide a chemical means of cross-linking. The peroxides are stable at normal processing temperatures but decompose to provide free radicals for cross-linking at higher temperatures in a post-processing vulcanization or curing reaction. An example of this type of cross-linking is illustrated in Figure 1. 2.

1.3.2 Vulcanization

The process by which a network of cross-links is introduced into an elastomer (molecular weight between 10 000 and 1 000 000) is called vulcanization [6]. Even though the chemistry of vulcanization is complex, its profound effects are clear i.e. it transforms an elastomer from a weak thermoplastic mass into strong, elastic, tough rubber. This may be illustrated by comparing the tensile strength of raw rubber (300psi) with vulcanized rubber (3000psi). The chemistry of vulcanization includes sulphur and nonsulphur vulcanization.

i) Sulphur vulcanization

The curing of rubber [6] with sulphur alone is quite slow and therefore accelerators such as thiazoles, e.g. 2-mercaptobenzothiazole, are usually used together with zinc oxide and a fatty acid. However, the mechanisms of sulphur vulcanization are not known in detail, but it is thought that the process is according to the scheme in Figure 1.3. Nevertheless, there may be many other possibilities. The zinc ions produced in the presence of the fatty acids appear to form chelates with the accelerator and sulphides, retarding and thus smoothing the course of the vulcanization process. Double bonds that may exist in the elastomer enhance the activity of the allylic hydrogen sites at which cross-linking occurs.

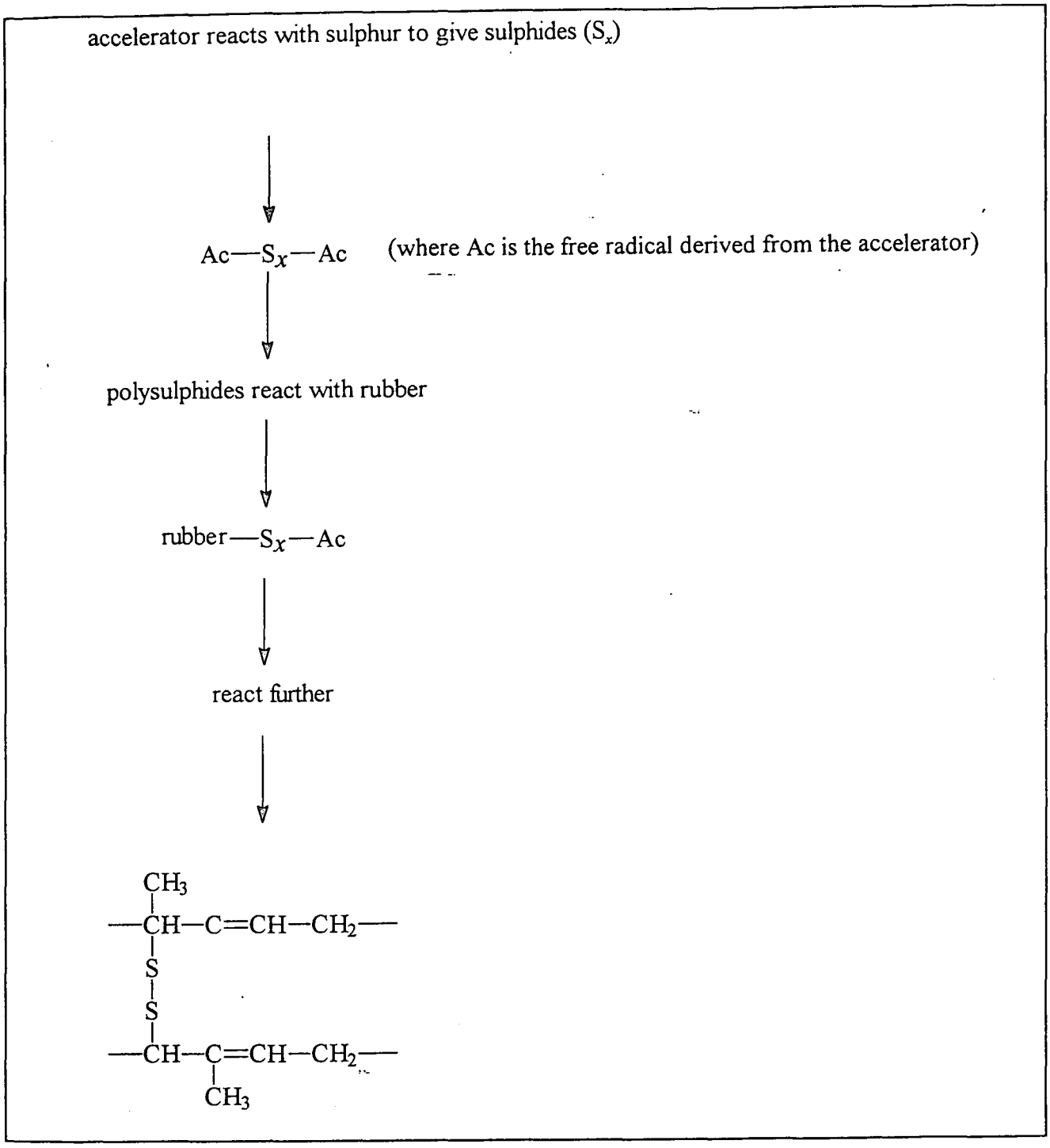

Figure 1.3 Scheme of accelerated sulphur vulcanization

ii) **Nonsulphur vulcanization**

The process occurs according to the following scheme [6]:

(a) A free radical R• is formed by the decomposition or oxidation of the curing agent.

(b) This free radical initiates vulcanization by abstracting a hydrogen atom from one of the α-methylene groups :

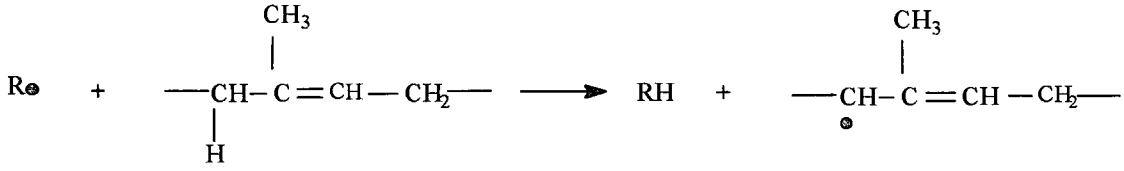

(c) The free radical then attacks a double bond in an adjacent polymer chain. This results in the formation of a cross-link and the regeneration of a free radical in a reaction analogous to propagation in an addition polymerization:

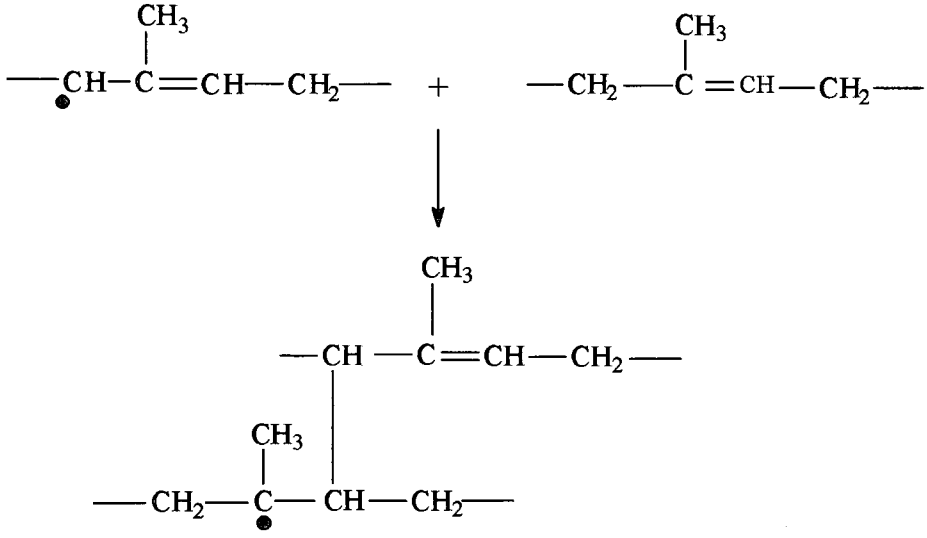

Chain transfer may also occur. Termination probably occurs by the reaction of the rubber free radical with a free radical fragment of the curing agent.

1.3.3 Radiation Cross-linking

When a molecular substance interacts with high energy radiation, its molecules are ionized [6]. Secondary electrons are emitted with relatively low speeds and thus produce many more ions. Within a fraction of a second, molecular rearrangements take place in the ions and excited molecules, accompanied by thermal deactivation or the dissociation of valence bonds. This leads to the production of ions or radicals whose lifetime depends on diffusion rates. The major effects in polymers arise from the dissociation of primary valence bonds into radicals. The dissociation of C-C and C-H bonds leads to degradation and cross-linking, which may occur simultaneously. Cross-linking is the predominant reaction in the irradiation of polystyrene, polyethylene and other olefin polymers, polyacrylates and their derivatives, and natural and synthetic rubbers. Radiation cross-linking has a beneficial effect on the mechanical properties of some polymers and is carried out commercially to produce polyethylene with enhanced form stability and resistance to flow at high temperatures.

1.3.4 Photocross-linking

Photocross-linking occurs when photo-active agents absorb light energy to form new chemical bonds [7]. It is accomplished by the use of photo-initiators, photocross-linking agents and photocross-linkable polymers, which represent the photo-active agent. Photocross-linking agents and photocross-linkable polymers are used primarily in photo-imaging applications, whereas photo-initiators are more broadly used in both photo-imaging and curing processes.

Photocross-linkable polymers possess chromophoric groups which can undergo light-induced chemical bonding with each other leading directly to cross-linked polymers. The chromophoric group may be incorporated into the polymer backbone or into a pendant from the backbone as illustrated by **(A)** and **(B)** below.

(A) $(OArCH{=}CHCOArO_2C\ )n$ → polychalcone

(B) $(CH_2CH\ )$ with pendant $O_2CCH{=}CHPh$ → poly(vinyl cinnamate)

Photo-initiated free-radical cross-linking copolymerization of methyl methacrylate (MMA) and ethylene glycol dimethacrylate (EGDM) has been investigated by Naghash *et al.* [8] to predict the final properties and structural characteristics of materials used in the application of dentistry, aspherical lenses, nonlinear optical materials and coatings. Polymerization initiated with ultraviolet light generated from a medium mercury lamp and the use of benzoin, benzoin methyl ether, benzoin ethyl ether and 2,2-dimethoxy-2-phenyl-acetophenone as photo-initiators produced gel formation by chain cross-linking. Gel point measurements were carried out by gravimetric technique and dilatometry. It was found that approximately 30% of the pendant vinyl groups were consumed by cyclization reactions. This effect reduced the accessibility of the radical centres and pendant vinyl groups from forming further multiple cross-linking and inhomogeneity.

Ultraviolet curing

Ultraviolet curing of coating and printing inks is based on photocross-linking by photo-initiated radical and cationic polymerization [7]. Monofunctional monomers polymerize to linear polymers, whereas a cross-linked polymer network requires monomers and oligomers.

Ultra-violet curing offers unique advantages over thermal curing for the following reasons :

a) rapid polymer network formation is accomplished by high intensity light sources.

b) heat sensitive substrates may be used.

Some advantages of this method were reported by Bellincampi *et al.* [9]. The properties of a versatile biomaterial (collagen) which is used in various tissue engineering applications were improved by cross-linking with UV irradiation. UV irradiation was the method selected as it could be used with ease, the synthesis time was half an hour as compared to 3-5 days when compared with other chemical methods. In addition, the covalent cross-link of the biomaterial excluded the introduction of potentially cytotoxic chemicals.

Other advantages include using substantially less energy with substantially lower solvent emissions than thermal curing, thereby minimizing air pollution. Ultraviolet curing lines are also substantially shorter therefore enabling rapid curing. Ultraviolet curable coatings and inks have a wide variety of applications as they are on glass, metal, paper, plastic and wood.

1.3.5 Sonochemistry

Ultrasound is a fairly new technique which may be used to modify polymers [10]. The two types of ultrasonic waves available are :

* high frequency (> 1 MHz) - low intensity
* low frequency - high intensity

High frequency waves are useful in providing information on relaxation phenomena such as segmental motion, conformational analysis, vibrational-translational energy interchange and polymer solvent interactions. Low frequency waves provide information on both polymerization and depolymerization.

Recent investigations [11] show that applying ultrasound to systems containing either a mixture of homopolymers or a mixture of polymer and monomers produce graft or block copolymers. A typical example of the production of a block copolymer is illustrated in Figure 1.4.

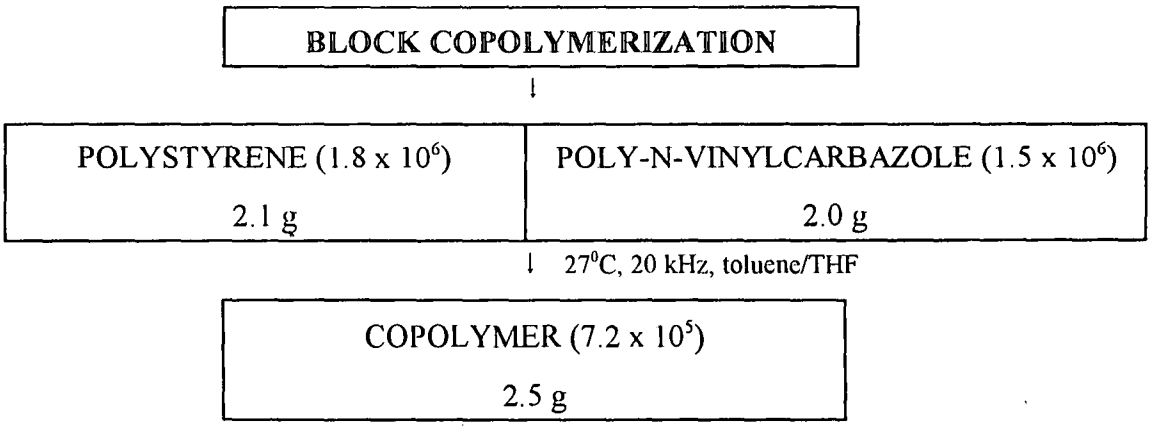

Figure 1. 4 Ultrasonic modification of polymers [10]

In addition, resin curing can be made more effective under ultrasonic conditions, since the heat distribution during the process of conventional mixing may be non-uniform, which can affect the overall efficiency of the thermally-induced chemical cross-linking reactions. In the case of peroxides, the ultrasonic energy can be used to break the catalyst bond and initiate reaction by liberation of free radicals. An example of an application in this field is the curing of the resin liners inserted into underground pipes to repair damage.

1.4 Previous work on cross-linking of long chain hydrocarbons

1.4.1 Wax cross-linking and dicumyl peroxide

Brink and Dressler [12] cross-linked a hard, Fischer-Tropsch wax using dicumyl peroxide (DCP) as the cross-linking agent. The cross-linking process was accomplished by stirring the two substances at 135 °C in a nitrogen atmosphere.

It was reported that the congealing points, gel permeation chromatography, infrared spectroscopy and tensile testing proved that the product had been cross-linked and that the elasticity had increased when compared to the starting material. However, the cross-link intensity depended upon the amount of DCP used. An excess of 1.1 mole of DCP per mole of wax gave insoluble and infusible hard, brittle gels. The other drawback observed was the side reactions that occurred during the cross-linking process.

A cross-linking mechanism was proposed and the efficiency of DCP as a cross-linking agent was established. Cross-linking was shown to be a suitable tool to modify the properties of higher paraffin waxes, even though large quantities of peroxides were required.

1.4.2 Cross-linking in resins

An epoxy resin (ER) was cross-linked/cured independently with two different types of cross-linking/curing agents i.e. a primary aromatic amine (AM) and phthalic anhydride (AN) to give [13] :

(i) ER + AM → AM-ER (amine cured epoxy resin)
(ii) ER + AN → AN-ER (anhydride epoxy resin)

Even though the authors did not perform the cross-linking themselves, they were able to establish that the resins were fully cross-linked by methods not stated and they also positively identified the dissimilarity between the two types of cured resins by measuring their cohesive energies. Since the strength between the two types of cross-links differed, it can be concluded that the type of curing agent selected is critical.

1.4.3 Cross-linking of polychloroprene with ZnO and MgO

The cross-linking of polychloroprene (PCR) was done in the presence of ZnO and MgO [14]. The reaction was followed by heating the samples in a Differential Scanning Calorimetric instrument, stopping the reaction at points along the thermogram, and analyzing the samples. Cross-linking was conducted by heating two sets of samples at a programmed rate. After cross-linking, the samples were rapidly removed and placed in liquid nitrogen to quench the reaction. One set of the samples were analyzed for Mg and Zn while the cross-link density was carried out on the other set. In PCR compounds, HCl was evolved during mixing and was trapped as $ZnCl_2$ or $MgCl_2$. $ZnCl_2$ catalyzes the cross-linking process as cross-linking commenced at lower temperatures in all compounds that contained $ZnCl_2$. In compounds having both ZnO and MgO, the bulk of the evolved HCl was trapped as $MgCl_2$. The cross-linking process was separated into two reaction sequences, one initiating at temperatures below 160 °C, and the second at temperatures above 180 °C. $ZnCl_2$ produced during mixing catalyzes the cross-linking reaction which, in turn, produces more $ZnCl_2$. MgO was found to retard the reaction by trapping HCl and delaying the buildup of $ZnCl_2$ during the mixing process.

1.4.4 Cross-linking of poly(methyl methacrylate)

Pavlinec *et al.*[15] cross-linked poly(methyl methacrylate) (PMMA) macromolecules with primary aliphatic diamines. The cross-linking was carried out between 140 and 200 °C, above the polymer glass transition temperature. This study presented the kinetics of PMMA cross-linking using polymer analogous reactions with small amounts aliphatic diamines. The reaction was carried out in sealed glass ampoules under a blanket of nitrogen in the molten state i.e. above the glass transition temperature of PMMA. A dissolution of the reaction product in chloroform was used to determine the conversion of PMMA polymer to the insoluble macromolecular network. The content of the bounded diamine was determined as the amount of nitrogen in the polymer. The chemical reactions of linear macromolecules with multifunctional compounds lead progressively from increasing the polymer molecular mass to insoluble cross-linked networks. The rate of polymer network formation was evaluated as the mass increase of the insoluble gel fraction in the sample.

1.4.5 Differential scanning calorimetry (DSC) of phenol-formaldehyde resin cure

The effects of temperature and humidity on the extent of phenol-formaldehyde (PF) resin cure was investigated by Wang *et al.*[16]. This study used DSC to determine the extent of PF resin cure after progressively extended exposures to precure treatments at different temperatures.

It was found that at 100 °C, the curing rate of aqueous resins decreased with increasing moisture dilution therefore prolonging the curing time. In addition, the curing rates increased as the temperature increased. In the calorimetry of PF resins, the exothermic peak at ~140 °C was identified as the curing/cross-linking peak and the area of this peak was used to quantify the resin cure.

1.4.6 Curing of epoxy resins

Two types of epoxy resins were cross-linked with 4,4' -diaminodiphenylmethane (DDM). The curing reaction was done isothermally at 70 °C. Changes during the thermal curing of the epoxides were observed for example the samples changed from a low-molecular-mass mixture to a highly cross-linked network. The molecular mobility was also noted to have decreased as the cure reaction proceeded. Younes *et al.*[17] used a variety of techniques that included viscometry, calorimetry, dielectric and mechanical relaxations, dilatometry, electrical and thermal conductivity, ultrasonic measurements and several spectroscopic methods such as infrared and Raman spectroscopy to demonstrate the complex procedure of this cross-linking process. The method applied were sensitive to the different physcial properties of the cross-linking epoxy system and they were therefore able to conclude that sol-gel and gel-glass transitions occurred in different ways.

1.4.7 Cross-linking in natural rubber

Natural rubber (NR) was cross-linked independently with sulphur and dicumyl peroxide (DCP) [18]. With a conventional sulphur vulcanizate at relatively high sulphur levels, polysulphidic bonds predominated, whereas approximately 90% of monosulphidic and disulphidic cross-links were formed with efficient vulcanization having a higher accelerator-to-sulphur ratio.

Carbon-carbon cross-linking was achieved by the use of DCP and electron radiation treatment [18]. An increase in the glass transition temperature was obtained with increasing peroxide. For the same amount of cross-linking agent, sulphur cured NR gave higher glass transition values, cross-linking densities and improved viscoelastic properties than the peroxide cured NR. It was therefore concluded that different types of cross-links had varied effects on the glass transition, viscoelastic properties and cross-link densities.

1.4.8 Curing of polyisoprene by radiation, peroxide and vulcanization

Polyisoprene (IR) networks were produced by four different types of cross-linking techniques [19] : high energy irradiation, peroxide curing, efficient vulcanization (EV) and conventional vulcanization (CV). The networks formed by the different methods were of varying cross-link density.

It was found that CV contained mostly polysulphidic cross-links and therefore had the highest tensile strengths than EV which had mainly monosulphidic cross-links. Peroxide cured networks with carbon-carbon cross-links had lower tensile strengths while irradiation networks also with carbon-carbon cross-links had even lower tensile strengths. The cross-link effectivity is therefore : CV>EV>DCP>irradiation. The cross-links were tested for its heterogeneity by methods of dynamic mechanical analysis, gel-solvent freezing point and scanning electron microscopy of fractured surfaces.

From the results obtained, it was observed that the heterogeneity had increased in the order : irradiation → DCP → EV → CV. It was concluded that the trend in network heterogeneity parallels the trend in physical properties, an increase in heterogeneity being associated with improved properties.

1.4.9 Cross-linking with DCP in the preparation of gas chromatograghy stationary phases

Much attention has been devoted recently to the preparation of gas chromatography (GC) stationary phases by using several types of free radical generators such as peroxides, gamma (γ) radiation and temperature [20]. The properties that were enhanced by cross-linking the of GC columns included film stability, solvent resistance, column efficiency and decreased column bleeding [20, 21, 22, 23].

For the enantiomeric separation of optically active compounds, polymeric chiral compounds were cross-linked with azo-*tert*-butane, DCP and γ radiation [20, 21]. Schomburg *et al.*[21] established that for effective cross-linking, the polymers should contain suitable groups such as vinyl because the vinyl groups facilitate cross-linking as in polysiloxane chemistry. Experiments with γ radiation and azo-*tert*-butane proved unsuccessful whereas 20% w/w DCP led to satisfactory cross-linking. Repeated experiments with such amounts of DCP gave reproducible results.

1.5 Analysis of cross-linked products

In order to gain an insight into the molecular structure of waxes, a variety of spectroscopic and thermal techniques may be used. The most useful of these techniques thus far are differential scanning calorimetry (DSC), thermogravimetry (TG), thermomechanical analysis (TMA), Fourier Transform Infrared (FTIR), nuclear magnetic resonance (NMR) and X-ray diffraction (XRD)[24]. NMR and XRD analyses were, however, not used in this study.

1.5.1 Thermal analysis

Thermal analysis (TA) is used to describe analytical experimental techniques which investigate the behaviour of a sample as a function of temperature. TA [24] refers to conventional TA techniques which include differential scanning calorimetry (DSC), differential thermal analysis (DTA), thermogravimetry (TG), thermomechanical analysis (TMA), and dynamic mechanical analysis (DMA). A typical DSC curve for a polymer is presented in Figure 1.5. The ability of these techniques allows for both quantitative and qualitative characterization.

The advantages of TA over other analytical methods can be summarized as follows:

(i) the sample can be studied over a wide temperature range using various temperature programmes

(ii) almost any physical form of sample (solid, liquid or gel) can be accommodated using a variety of sample vessels or attachments

(iii) a small amount of sample (0.1μg - 10mg) is required

(iv) the atmosphere in the vicinity of the sample can be standardised

(v) the time required to complete an experiment ranges from several minutes to several hours.

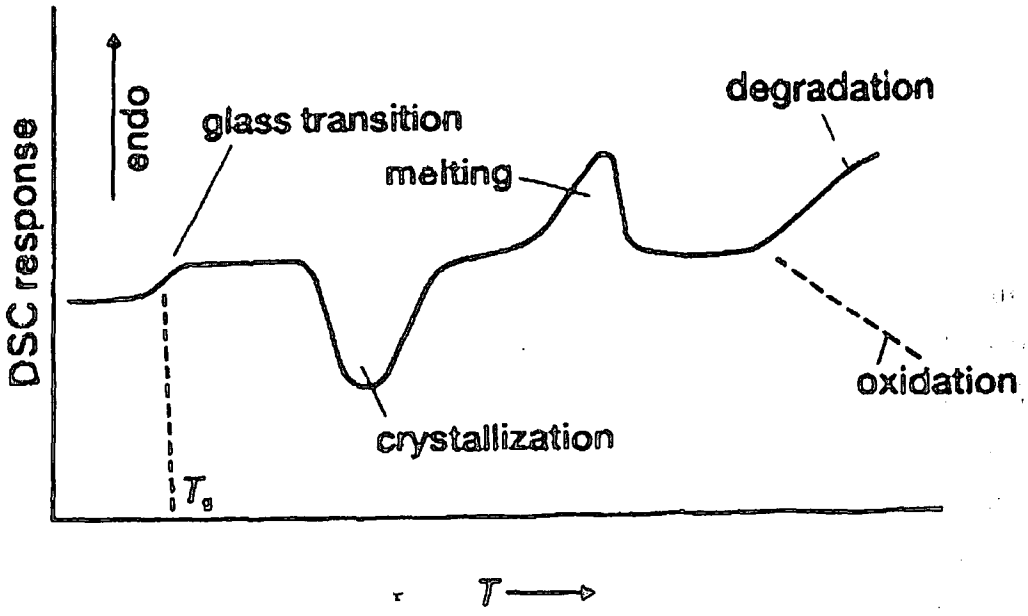

Figure 1.5 Typical DSC curve for a polymer

In polymer science, preliminary investigations of the sample transition temperatures and decomposition characteristics is routinely performed using TA before any spectroscopic analysis. However, TA data is indirect and must be collated with results from spectroscopic measurements before the molecular processes responsible for the observed behaviour can be elucidated. Spectroscopic instruments that may be used are NMR, Fourier transform infrared (FTIR) and X-ray diffraction. Irrespective of the rate of temperature change, a sample studied using a TA instrument is measured under non-equilibrium conditions, and the observed transition temperature is not the equilibrium transition temperature.

The recorded data is influenced by the following experimental parameters:

(i) sample dimensions and mass

(ii) the heating/cooling rate

(iii) the nature and composition of the atmosphere in the region of the sample

(iv) the thermal and mechanical history of the sample.

The precise sample temperature is unknown during a TA experiment as the thermocouple which measures the sample temperature is rarely in direct contact with the sample. Even when in direct contact with the sample, the thermocouple cannot measure the magnitude of the thermal gradient in the sample, which is determined by the experimental conditions and the instrument design. The sensitivity and precision of TA instruments to the physical and chemical changes occurring in the sample are relatively low compared to spectroscopic techniques. TA is not a passive experimental method, as the high-order structure of a sample, for example crystallinity, may change during the measurement. On the other hand, samples can be aged, cured or their previous thermal history erased using these instruments.

1.5.1.1 Differential scanning calorimetry (DSC)

Heat flow DSC

The temperature difference between the sample and reference is measured as a function of temperature or time, under controlled temperature conditions [24]. The temperature difference is proportional to the change in the heat flux (energy input per unit time). In the conformation the thermocouples are attached to the base of the sample and reference holders. A second series of thermocouples measure the temperature of the furnace and of the heat sensitive plate. During a phase change, heat is absorbed or emitted by the sample, altering the heat flux through the heat-sensitive plate. The variation in heat flux causes an incremental temperature difference to be measured between the heat-sensitive plate and the furnace. Temperatures greater than 727 °C may be measured depending on the design of the furnace.

Power compensation DSC

The sample and reference holders are individually equipped with resistance sensors, which measure the temperature of the bases of the holders, and resistance heaters [24]. If a temperature difference is detected between the sample and the reference, due to a phase change in the sample, energy is supplied until the temperature difference is less than a threshold value (< 0.01 °C). The energy input per unit time is recorded as a function of temperature or time. The temperature range of a power compensation DSC system is between -160 and 730 °C.

1.5.1.2 Thermogravimetry (TG)

TG is the branch of thermal analysis which examines the mass change of a sample as a function of temperature in the scanning mode or as a function of time in the isothermal mode [24]. Not all thermal events bring about a change in the mass of the sample, e.g. melting, crystallization or glass transition. Some very important exceptions are desorption, absorption, sublimation, vaporization, oxidation, reduction and decomposition. TG is used to characterize the decomposition and thermal stability of materials under a variety of conditions, and to examine the kinetics of the physico-chemical processes occurring in the sample. The mass change characteristics of a material are strongly dependent on the experimental conditions employed. Factors such as sample mass, volume and physical form, shape and nature of the sample holder, the nature and pressure of the atmosphere in the sample chamber and the heating rate all have important influences on the characteristics of the recorded TG curve. TG cannot be considered as a black box technique where fingerprint curves are obtained irrespective of the experimental conditions. Establishing the optimum conditions for TG analysis frequently requires many preliminary tests . It is essential for accurate TG work that the experimental conditions be recorded and that within a given series of samples the optimum conditions be standardised and maintained throughout

the course of the experiments. Only then can the TG curves from different experiments be compared in a meaningful way.

1.5.2 Fourier-transform infrared spectroscopy (FTIR)

The most common option to measure absorption spectra of organic substances is the modern, non-dispersive FTIR spectrophotometer which operates in the region 4000-400 cm $^{-1}$ [25]. One of the essential components of the FTIR is the interferometer. The design of the optical pathway produces a pattern called a interferogram. An interferogram is essentially a plot of intensity versus time that contains all the frequencies which make the infrared spectrum. The sample preparation is virtually the same as used in dispersive infrared i.e. KBr disc or Nujol mull for solids and salt plates for liquids.

1.5.3 FTIR - photoacoustic spectroscopy (PAS-FTIR)

The main sample handling problem in FTIR analysis of solid and semi-solid materials is that nearly all materials are too opaque in their normal forms for direct transmission analysis in the mid-infrared spectral region [26]. Traditionally, the opacity problem has been remedied by reducing the optical density of samples to a suitable level by various methods of sample preparation. This approach, however, leaves much to be desired due to the time and labour involved, the risk of sample alteration and preparation errors, and the destructive nature of the process. The most broadly applicable mid-infrared solution to the opacity problem is therefore a newly developed technique called photoacoustic spectroscopy (PAS).

The PAS cell is an attachment to the FTIR. The photoacoustic signal is generated when infrared radiation absorbed by the sample converts into heat within the sample. This heat diffuses from the sample surface into an adjacent gas atmosphere. The thermal expansion of this gas produces the photoacoustic signal.

The signal generation process is automatic, reproducible and one that isolates a layer extending beneath the sample's surface which has suitable optical density for analysis without physically altering the sample. PAS directly measures the absorbance spectrum of the layer without having to infer a reflection or transmission measurement.

CHAPTER TWO

EXPERIMENTAL

2.1 Materials

The materials used were three types of paraffin waxes (waxes 1- 3) supplied by Schümann-Sasol. The process of wax production is schematically described in Figure 2.1. Coal is mixed with steam and oxygen under high pressure to produce a gas mixture and a large amount of ash [3]. The gas mixture consists mainly of CO, H_2 and CH_4 together with impurities such as H_2S. Impurities are removed and the CO and H_2 are then reacted in the presence of a catalyst. The general reactions are :

$$n(CO + 2H_2) \rightarrow C_nH_{2n} + nH_2O \quad (1)$$

$$n(CO + 2H_2) + H_2 \rightarrow C_nH_{2n+2} + nH_2O \quad (2)$$

$$n(2CO + H_2) \rightarrow C_nH_{2n} + nCO_2 \quad (3)$$

$$n(2CO + H_2) + H_2 \rightarrow C_nH_{2n+2} + nCO_2 \quad (4)$$

The hydrocarbon chain is built up by the first and third reactions and it is terminated either as an olefin or as a paraffin by the second and fourth reactions. Products where $n > 23$ are classified as waxes.

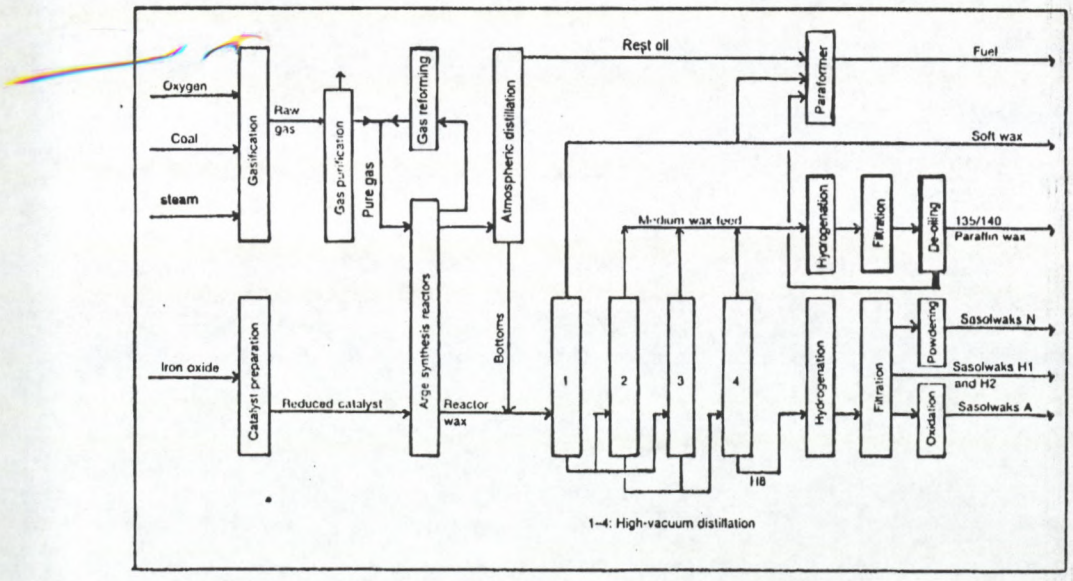

Figure 2.1 Flow diagram of wax production

2.1.1 Wax 1

Wax 1 is a typical hard oxidized Fischer-Tropsch wax that exhibits some properties of microcrystalline waxes [3, 27]. This wax consists of long-chain acids, esters, alcohols, ketones and some unreacted paraffins (alkanes). It is also an emulsifiable wax which has good solvent-retention properties that allows it to be applied in polishes and coatings. Some of it characteristics are listed in Table 2.1.

2.1.2 Wax 2

Wax 2 is a paraffinic Fischer-Tropsch wax with an average molecular formula of $C_{23}H_{48}$ [3, 27]. This medium melting point wax has chains that are about 84% unbranched and is used mostly in candle molding and polishes. Some characteristics of this wax are seen in Table 2.2.

Table 2.1 Properties of Wax 1

PROPERTY	VALUE
Average molecular mass	660
Boiling point	239 °C
Congealing point	80 °C minimum
Softening point	100 °C
Physical appearance	off-white waxy beads
REACTIVITY DATA	
Reactions : reacts at high temperatures with oxidizing agents	
Thermal decomposition : occurs at ± 250 °C forming hydrocarbon gases	
Air and water : no reaction	

2.1.3 Wax 3

Wax 3 is a high molecular mass Fischer-Tropsch wax with a narrow carbon number distribution ranging from C_{38} -C_{93} [3, 27]. It is chemically inert and is free of aromatics. Table 2.3 shows some of its properties.

Table 2.2 Properties of Wax 2

PROPERTY	VALUE
Average molecular mass	440
Congealing point	65-70 °C
Physical appearance	off-white waxy beads
REACTIVITY DATA	
Reactions : reacts at high temperatures with oxidizing agents	
Thermal decomposition : occurs at ± 250 °C forming hydrocarbon gases	
Air and water : no reaction	

Table 2.3 Properties of Wax 3

PROPERTY	VALUE
Average molecular mass	1300
Congealing point	102-108 °C
Physical appearance	hard white waxy beads
REACTIVITY DATA	
Reactions : reacts at high temperatures with oxidizing agents	
Thermal decomposition : occurs at ± 250 °C forming hydrocarbon gases	
Air and water : no reaction	

2.2 Cross-linking agents

Cross-linking or curing agents are the chemical substances that are used to create a network or branches from straight paraffinic chains. The curing agents dicumyl peroxide and potassium peroxodisulphate were selected as they are strong oxidizing agents that may be used as polymerization catalysts or vulcanization agents [5].

2.2.1 Dicumyl Peroxide (DCP)

Curing agents such as peroxides are often used as initiators [13, 20-23] in some polymer reactions. Peroxide-initiated polymerization is thought to proceed in the following manner [28]:

$$R\text{-}O\text{-}O\text{-}H \rightarrow R\text{-}O^{\circ} + {}^{\circ}O\text{-}H \quad (1)$$

$$R\text{-}O^{\circ} + H_2C{=}CH_2 \rightarrow R\text{-}O\text{-}H_2C\text{-}CH_2{}^{\circ} \quad (2)$$

$$R\text{-}O\text{-}H_2C\text{-}CH_2{}^{\circ} + H_2C{=}CH_2 \rightarrow R\text{-}O\text{-}H_2C\text{-}CH_2\text{-}H_2C\text{-}CH_2{}^{\circ} \quad (3)$$

In (1), the peroxide is assumed to have broken a covalent bond to produce the free radical $R\text{-}O^{\circ}$. In (2), the radical combines with an ethylene molecule to form a new free radical which is one $-CH_2-CH_2-$ unit greater than the original. Chain propagation thus continues, (3), and a giant molecule is progressively built up until the free radical is destroyed by combining with other free radicals or by reacting with some chemical inhibitor.

DCP also known as bis(α, α-dimethylbenzyl) peroxide has the following properties [5]:

Molecular mass	:	270,35 g mol^{-1}
Molecular formula	:	$C_{18}H_{22}O_2$
Melting point	:	37- 40 ^{0}C
Supplier	:	Merck
Structure	:	

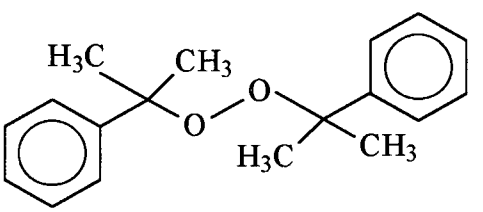

2.2.2 Potassium peroxodisulphate (PPS)

PPS also known as potassium persulphate are white, water soluble crystals that decompose below 100 °C. The peroxodisulphate ion decomposes into free radicals, which are initiators for numerous chain reactions [5, 29]. The principal use of the peroxodisulphate salt is as initiators for olefin polymerization in aqueous systems in the manufacturing process of polyacrylonitrile and its copolymers.

PPS has the following properties :

Molecular mass	:	271.31 g.mol-1
Molecular formula	:	$K_2S_2O_8$
Decomposition temperature	:	< 100 °C
Refractive index (n)	:	1.461, 1.467, 1.4695
Crystalline form	:	triclinic
solubility (g/100cc)	:	1.75 ° cold water, 5.20 ° hot water
Density	:	2.477 kg dm^{-3}
Supplier	:	BDH Lab Supplies, Poole, England

2.3 Differential scanning calorimetry (DSC)

2.3.1 Calibration

Standard reference materials such as indium or tin, are used to calibrate the temperature and energy scales of DSC instruments [24]. After calibration, the characteristic temperatures and the enthalpy associated with a phase change can be measured for any sample. The upper limit for the precision of all instruments is set by the accuracy of the calibration. Temperature calibration is carried out using the melting temperature of metals whose purity is greater than 99.99%. The reason being that laboratory grade chemicals may contain trace amounts of impurities which has a large effect on the observed melting temperature. Tiny indium pellets (1-2mg) were heated using a temperature program for calibration of DSC . The temperature for indium obtained was 156 °C and was agreeable with literature value of 157 °C [29].

2.3.2 Instrument - DSC

Model	:	Mettler T C 11 TA Processor
		Mettler DSC 20 standard cell
Computer software	:	GraphWare TA72 PS.5
Plotter	:	Roland DXY 1150

2.3.3 Experimental parameters

Nitrogen flow	:	3 units (1unit = 28.81 mL min^{-1})
Sample size	:	~20 mg
Pans	:	aluminium, 40 µL (Mettler)
Start temperature	:	30 °C
Heating rate	:	10 °C min^{-1}
End temperature for DCP	:	215 °C
End temperature for PPS	:	240 °C

2.4 Thermogravimetry (TG)

2.4.1 Calibration

The TG was calibrated with metal alloys which are ferromagnetic at low temperatures but which lose their ferromagnetism at a well defined Curie point [30]. The metals selected for calibration were : nickel (353 °C), alumel (163 °C).

2.4.2 Instrument

Model	:	Mettler T G 50 Thermobalance
		Mettler TC 10 A TA Processor
Computer software	:	GraphWare TA72 PS.5
Plotter	:	Roland DXY 1150

2.4.3 Experimental parameters

Nitrogen flow	:	3 units (1 unit = 28,81 mL min^{-1})
Pans	:	aluminium, 40 µL (Mettler)
Start temperature	:	30 °C
Heating rate	:	10 °C min^{-1}
End temperature for DCP	:	215 °C
End temperature for PPS	:	240 °C

2.5 FOURIER - TRANFORM INFRARED (FTIR)

The Fourier-transform infra-red was calibrated using a film of polystyrene that was supplied with the instrument. The polymer film was scanned and the wave numbers were compared to that to that of the given. Before each run, a background of air was done. In addition, the energy of the laser beam was monitored to ensure optimum laser efficiency. Wax samples, initially mixed with respectively 10%, 30% and 50% of curing agent, were cured thermally from 30 to 240 °C (in the case of PPS) or 215 °C (in the case of DCP) in a nitrogen atmosphere. KBr discs containing the cured samples were thereafter prepared and run in the FTIR.

2.5.1 Instrument

Model	:	Nicolett 410 Impact Series
Plotter	:	Roland DXY 1250

2.5.2 Parameters

Resolution	:	4 and 8
Detector	:	TGS
Background	:	air
Scan speed	:	0.12 $m.s^{-1}$
Number of scans	:	8
Potassium bromide	:	spectroscopic grade

2.6 Gel Content

The gel content produced as a result of cross-linking may be determined by extracting the uncross-linked wax with solvents such as decahydronaphthalene or xylene [31]. Wax samples, initially mixed with respectively 10%, 30% and 50% of curing agent, were cured thermally from 30 to 240 °C (in the case of PPS) or 215 °C (in the case of DCP) in a nitrogen atmosphere. The cured samples were weighed and inserted into a pre-weighed wire mesh (38μm). The samples were inserted in a Soxhlet apparatus [32] and heated for six hours. The Soxhlet apparatus is shown in Figure 2.2. The cured sample in the wire mesh is placed in section B of the Soxhlet. A flat bottom flask (200mL) containing 150 mL of toluene was fitted below the Soxhlet apparatus and a double surface type reflux condenser was placed on top. When the solvent boils, the vapour passes up through the tube C where it condenses. When the Soxhlet

cup that contains the mesh is full, as indicated by D, it siphons over into the flask, taking with it the substance which has dissolved in it. The extracted samples were removed from the Soxhlet apparatus and vacuum dried overnight before weighing.

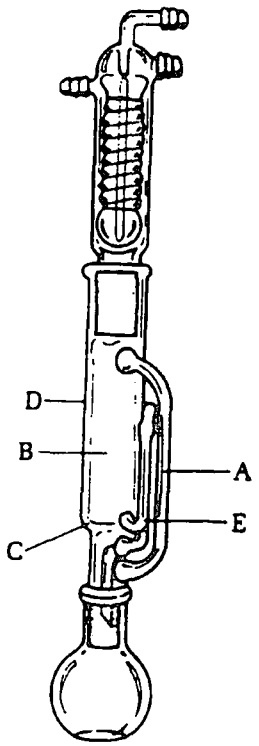

Figure 2.2 Soxhlet apparatus used for gel content

The percent gel was calculated as follows [31]:

Step 1 : % Extract = (mass loss during extraction/ sample mass) X 100

= [(W4 - W3)-W2 / W1)] X 100

where :

W1 = mass of sample

W2 = mass of mesh pouch and sample pan

W3 = mass of mesh pouch, sample and pan after extraction

W4 = mass of mesh pouch, sample and pan before extraction

Step 2 : Gel = 100 - % extract

2.6.1 Reagents and apparatus

Toluene	:	spectroscopic grade
Volume	:	150 mL
Soxhlet	:	as per Fig. 2.2
Heating mantle	:	J P Selecta , S A
Heat setting	:	2
Balance	:	Mettler 160

CHAPTER 3

RESULTS & DISCUSSION

3.1 Analysis of DCP

3.1.1 DSC and TG

Figure 3.1 represents the DSC and TG curves of DCP. The endotherm at approximately 38 °C shows the melting of DCP and is in good agreement with the literature value of 37 to 40 °C. The decomposition of the DCP is reflected by the exotherms between 140 ° and 200 °C. The peak shoulder suggests that the decomposition occurs in more than one step. However, this is not evident in the TG curve, which only shows one mass loss step in this temperature range.

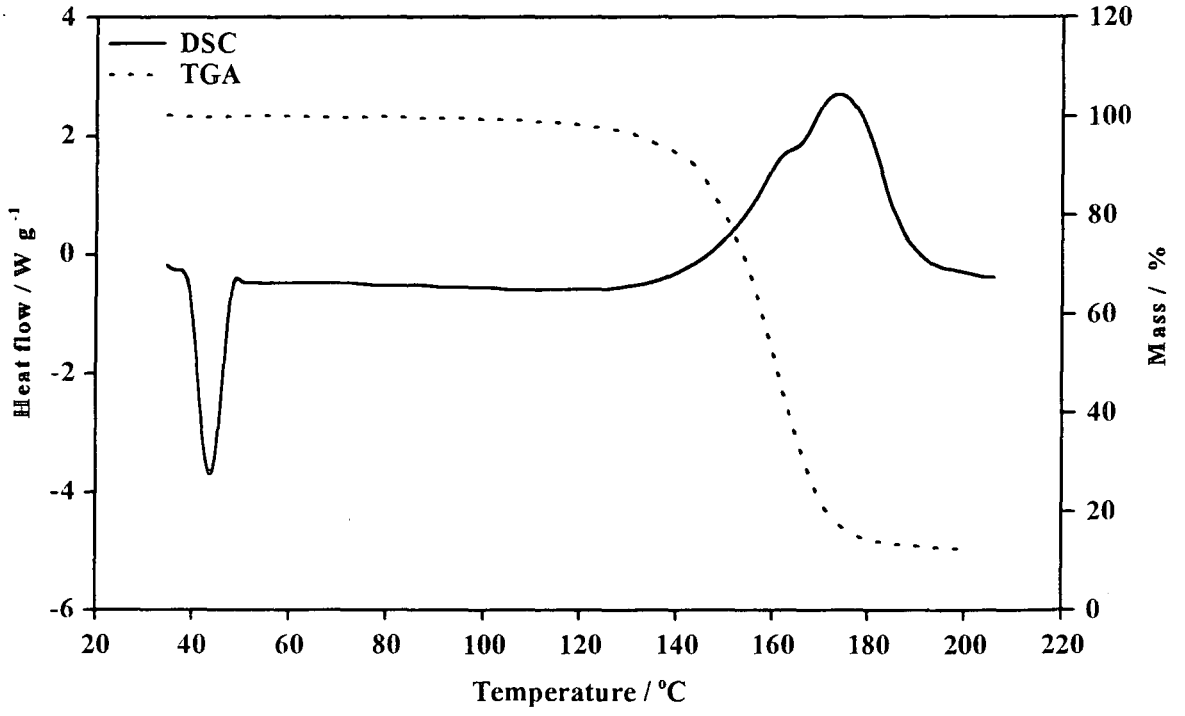

Figure 3.1 DSC and TG curves for dicumyl peroxide (DCP)

3.1.2 FTIR

The FTIR spectrum of DCP is shown in Figure 3.2 (b). A summary of the absorption bands is listed in Table 3.1.

Table 3.1. Summary of FTIR bands for DCP

Bands / cm $^{-1}$	Comments
3100 - 3000	sp^2 C - H stretch
2000 - 1750	monosubstituted
1600 - 1400	aromatic C=C
1300 - 1000	C-O stretch
800 - 600	Out-of-plane bending, monosubstituted

The bands occurring between 3100 and 3000 cm $^{-1}$ are due to the sp^2 C - H stretch in aromatic rings as they occur at values greater than 3000 cm^{-1} [25]. The monosubstituted ring pattern is confirmed by the many weak combination and overtone absorptions appearing between 2000 and 1750 cm^{-1} and the strong out-of-plane absorptions between 800 and 600 cm $^{-1}$. The absorptions in the region 1600 to 1400 cm $^{-1}$ are characteristic of the aromatic C=C stretch. The C-O bond stretch can be seen by the strong absorption occurring between 1300 and 1000 cm^{-1} .

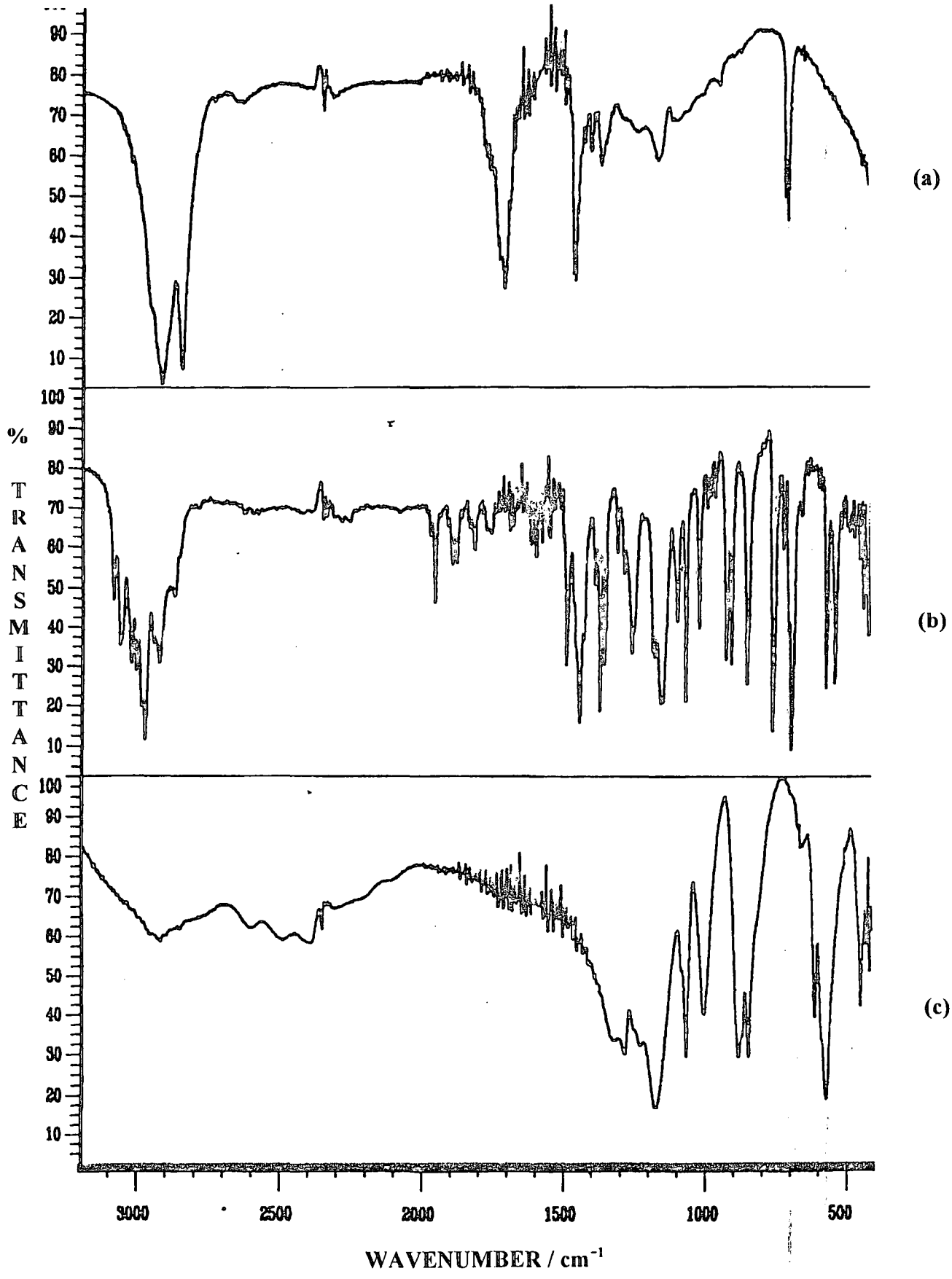

Figure 3.2 FTIR spectra of (a) untreated wax 1, (b) pure DCP, and (c) pure PPS

3.2 Analysis of PPS

3.2.1 DSC and TG

The thermal effects of pure potassium persulphate (PPS) are seen in Figure 3.3. The DSC curve shows an immediate change in heat capacity at the start temperature, followed by a weak endotherm at about 140 °C and a strong exotherm between 200 and 250 °C. The immediate reaction occurring at about 30 °C and the weak endotherm are reproducible, but cannot be explained because of a lack of available information on the thermal decomposition mechanism of PPS. The exotherm between 200 and 250 °C is the decomposition of PPS into K_2SO_4, which is the decomposition product according to literature [29]. The decomposition temperature does, however, not correspond with the value given in the CRC handbook of Chemistry and Physics. Thermogravimetric analysis of PPS shows a small mass loss starting at 200 °C which is the same as the start temperature of the decomposition exotherm in the DSC curve. It was, however, not possible to draw a correlation between the observed mass loss and that expected for the decomposition reaction mentioned above.

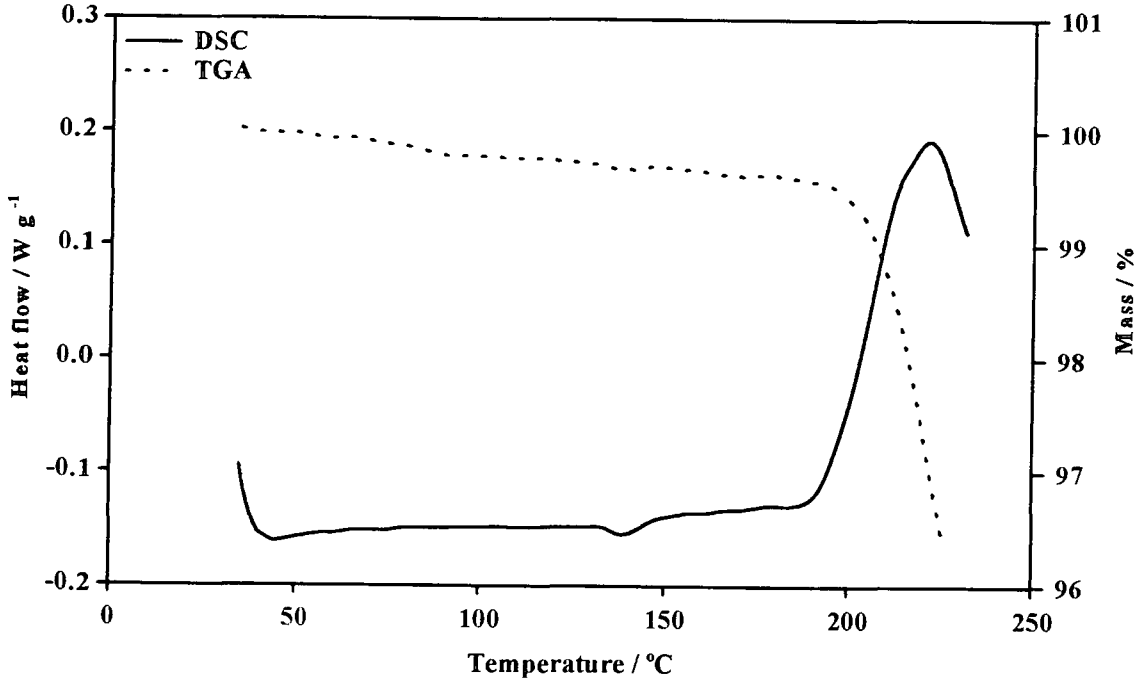

Figure 3.3 DSC and TG curves of potassium persulphate (PPS)

3.2.2 FTIR

The FTIR spectrum of PPS is shown in Figure 3.2 (c). Table 3.2 is a summary of the absorption bands.

Table 3.2 Summary of FTIR bands for PPS

Bands / cm^{-1}	Comments
1190 - 1050	S=O stretch
1000 - 550	S-O stretch

The strong band ocurring at 1190 cm^{-1} is the symmetric stretch of S=O [25]. Strong absorption at 1050 cm^{-1} may be the S=O stretch that is typical in sulphoxides. The bands appearing between 1000 and 550 cm^{-1} are indicative of the S-O stretch.

3.3 Cross-linking of wax 1 in presence of DCP

3.3.1 DSC

Figure 3.4 represents the DSC curves of the untreated wax and 10, 30 and 50% m/m mixtures of DCP with the wax. In the DSC curve of the untreated wax, the endotherm starting at approximately 50 °C reflects the melting of the wax. The DSC curves of wax mixed with different amounts of DCP show low-temperature endotherms increasing in size, which reflects the melting of increasing amounts of DCP in the samples. The DCP melting endotherm in the 10 % mixed wax is not clearly defined as the concentration of the DCP is too small. The exotherms between 150 and 200 °C increase in size with increasing DCP content and reflect the expected decomposition of the DCP followed by the cross-linking of the wax. These peaks are, however, not well resolved indicating the interrelation of DCP decomposition and wax cross-linking.

Samples of wax 1, reheated after initial heating and cooling, show considerably smaller wax melting endotherms, while the DCP melting endotherms and the exotherms are absent (Fig. 3.5). The ratios of the sizes of the reheat wax melting endotherms to that of the initial wax melting endotherms are inversely proportional to the amount of DCP mixed into the wax, confirming increased cross-linking of the wax in the presence of increased amounts of DCP.

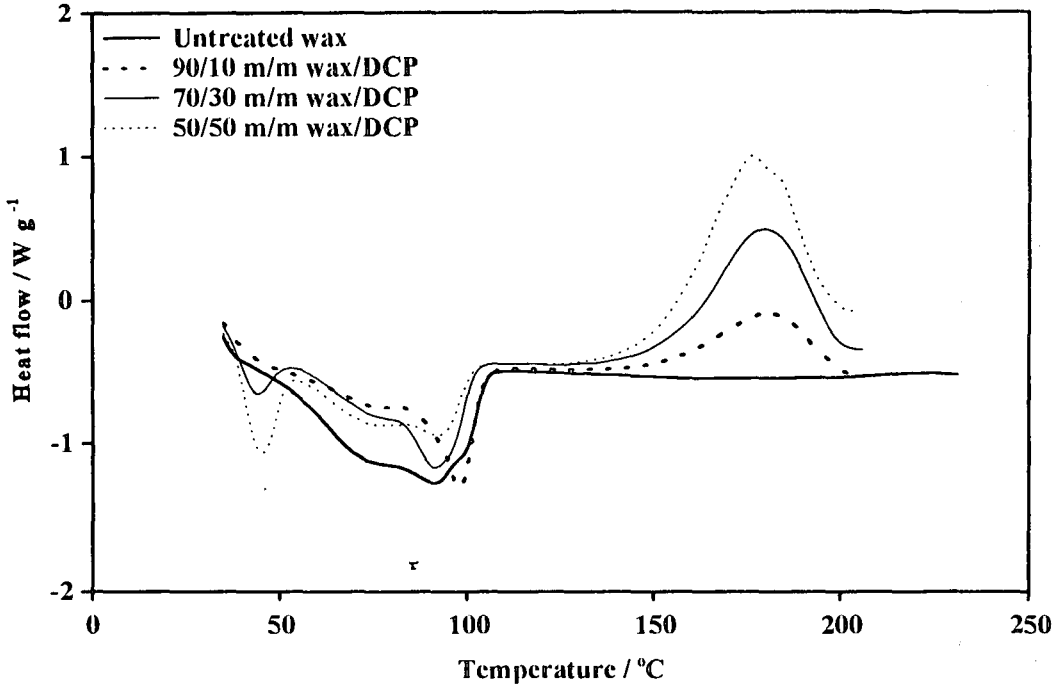

Figure 3.4 DSC curves of untreated wax 1 as well as samples mixed with different amounts of DCP

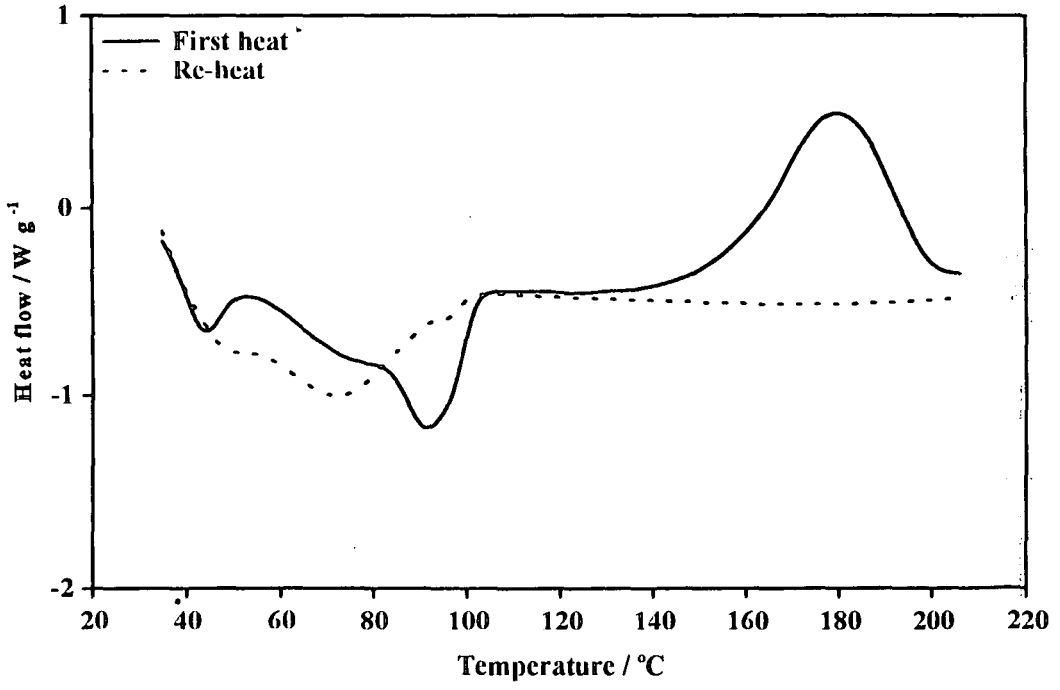

Figure 3.5 Heat and reheat curves of 70/30 m/m wax 1/DCP

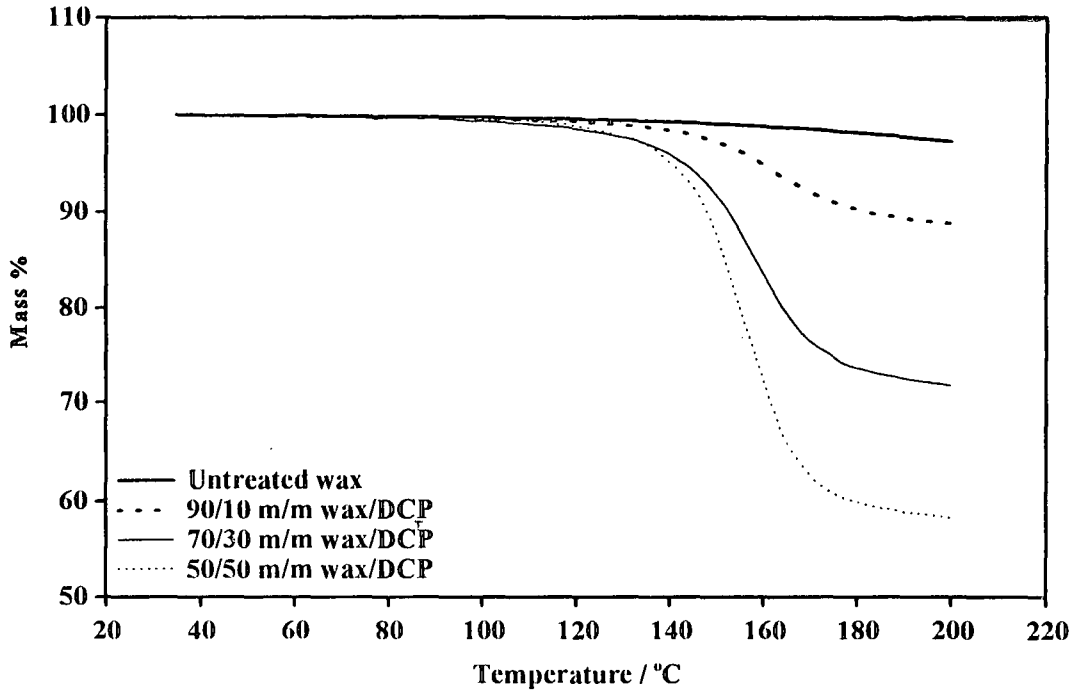

Figure 3.6 **TG curves of untreated wax 1 as well as samples mixed with different amounts of DCP**

3.3.2 TG

Figure 3.6 represents the TG curves of the untreated wax and 10, 30 and 50% m/m mixtures of DCP with the wax. The untreated wax shows only a small mass loss towards the end of the curve. A gradual mass loss is noted for the mixtures at approximately 160 °C. The trend observed in these reactions is that as the amount of DCP increases, the mass loss increases showing that DCP decomposition products evaporates during and after cross-linking initiation.

3.3.3 FTIR

The FTIR spectra of the 10, 30 and 50% DCP is shown in Figure 3.7. Figure 3.2 (a) represents the FTIR spectrum of the untreated wax. Table 3.3 is a summary of the absorption bands due to the untreated wax and the mixtures.

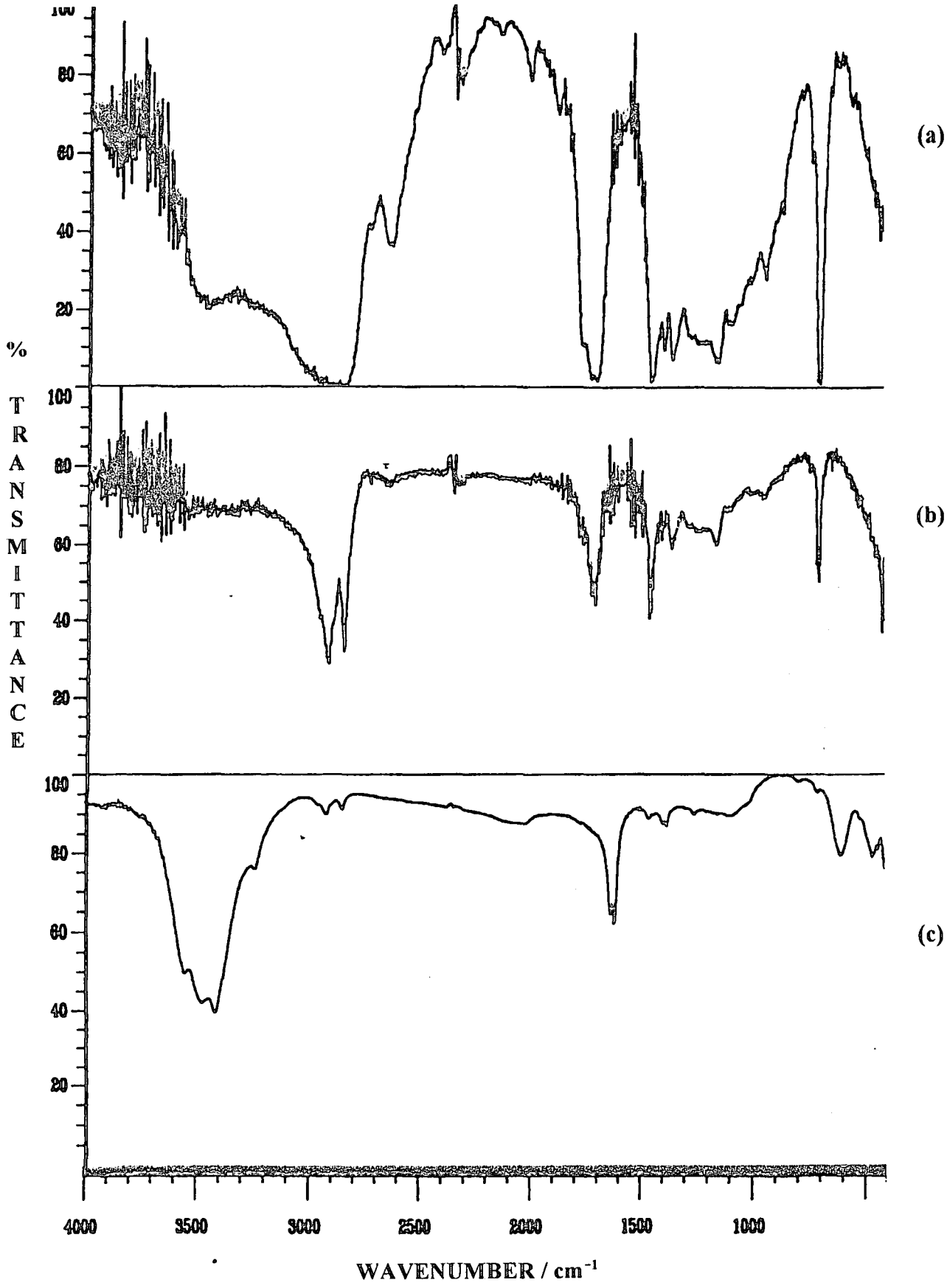

Figure 3.7 FTIR spectra of (a) wax 1 + 10% DCP, (b) wax 1 + 30% DCP, and (c) wax 1 + 50% DCP

Table 3. 3 Summary of FTIR bands for untreated and treated wax 1

Untreated wax	90/10 m/m wax/DCP	70/30 m/m wax/DCP	50/50 m/m wax/DCP
			3550-3400 cm^{-1}
2950-2850 cm^{-1} C-H stretch	3300-2850 cm^{-1} broad band	2900-2850 cm^{-1} C-H stretch	2950-2850 cm^{-1} C-H stretch
	2650 cm^{-1} C-H stretch		
	2000 cm^{-1} unknown		
1710 cm^{-1} C=O	1710 cm^{-1} C=O	1710 cm^{-1} C=O	1650 cm^{-1} C=O
1475 cm^{-1} CH_2 bending	1475 cm^{-1} CH_2 bending	1475 cm^{-1} CH_2 bending	1475 cm^{-1} CH_2 bending
1410-1375 cm^{-1} CH_3 bending	1400-1375 cm^{-1} CH_3 bending	1400-1375 cm^{-1} CH_3 bending	1400-1375 cm^{-1} CH_3 bending
1175 cm^{-1} C-CO-C	1150 cm^{-1} C-CO-C	1150 cm^{-1} C-CO-C	1250 cm^{-1} C-CO-C
710 cm^{-1} out-of-plane bending	750 cm^{-1} out-of-plane bending	750 cm^{-1} out-of-plane bending	600 cm^{-1} out-of-plane bending

The C-H stretching and bending regions are two of the most difficult regions to interpret. The C-H stretching region, which ranges from 3300 to 2750 cm^{-1}, is normally used. The physical constants that are used for *sp* -, sp^2 - and sp^3 - hybridized carbons are 3300 cm^{-1}, ~3100 cm^{-1} and ~2900 cm^{-1} respectively.

The spectrum of the untreated wax is typical of simple paraffins [25]. C-H stretching is accounted for in the region between 2900 to 2800 cm^{-1}. Wax 1 was said to contain long-chain acids, esters, alcohols and ketones. The absence of -O-H absorbance between 3650 to 3300 cm^{-1} indicates that no alcohol or acid groups are present. However, the carbonyl group present in acids, esters and ketones absorbs strongly in the range from 1850 to 1650 cm^{-1}. Since the C=O stretching frequency is sensitive to attached atoms, the common funtional groups already mentioned absorb at characteristic values [25].

Therefore the band at around 1700 cm $^{-1}$ is due to C=O bond in ketones and esters, while the C-O bond stretching absorption in esters is found between 1300 and 1000 cm $^{-1}$. CH_2 and CH_3 bending vibrations could be accounted for at 1475 and 1375 cm $^{-1}$. The band at around 700 cm $^{-1}$ is characteristic of long chains [25].

The bands in the region 3500 to 3400 cm $^{-1}$ appearing in the wax treated with 50% m/m DCP are indicative of only aromatic sp^2 C-H vibrations as it occurs at values greater than 3000 cm $^{-1}$. The bands ocurring between 2950 and 2850 cm $^{-1}$ are the sp^3 C-H stretching vibrations. These absorptions decrease in intensity with increasing DCP content, which confirms the formation of cross-links between the different wax chains.

The broad band around 3500 cm $^{-1}$ in Fig. 3.7 (a) includes the C-H stretch. Its broadness is characteristic of an O-H presence. This seems to have shifted the band that appears between 2850 cm $^{-1}$ and 2650 cm $^{-1}$. This spectrum includes a weak band at 2000 cm $^{-1}$ which is not present in Fig. 3.2 (a) or Fig. 3.7 (b) and (c), and which cannot be explained with the available information. The band at 1710 cm $^{-1}$ is characteristic of C=O stretching in ketones. Conjugation moves the absorption to a lower frequency and this could explain the shift in Fig. 3.7 (c). Again there is a decreasing absorption intensity with increasing DCP content, indicating functionalisation followed by cross-linking.

The presence of CH_2 and CH_3 groups is determined by analyzing the region between 1465 and 1370 cm $^{-1}$. The bands in this region, observed for both the treated and untreated waxes, could be due to the CH_2 scissoring and CH_3 bending respectively. The intensities of these bands again decrease as the DCP concentration increases.

The bending of C-CO-C band in ketones normally appears as a medium intensity peak between 1300 and 1100 cm $^{-1}$. In this case there is also a decreasing intensity and a slight shift to a higher frequency with increasing amount of DCP.

3.4 Cross-linking of wax 1 in presence of PPS

3.4.1 DSC

Figure 3.8 represents the DSC curves of the untreated wax and 10, 30 and 50% m/m mixtures of potassium persulphate (PPS) with the wax. Melting of the untreated wax is seen as a broad endotherm

in the temperature range 50 to 100 °C. The presence of PPS, however, changes the melting characteristics of the wax, as seen in the shapes of the wax melting endotherms and the positions of their maxima. In all three treated samples the melting endotherms form sharper peaks with maxima at about 100 °C. For these samples the exotherms between 185 °and 240 °C are similar to that observed for pure, unmixed PPS (Fig. 3.3), but the peak maxima are at somewhat lower temperatures. The decomposition exotherm also increases in size with increasing PPS content, but this decomposition of PPS does not give rise to cross-linking of the wax, as will be seen later in the discussion.

Reheating the PPS treated wax samples showed an interesting phenomenon (Fig. 3.9). There is a slight change in the shape of the wax melting endotherm and the position of its maximum, but the total area remained approximately the same. Two endotherms, the first considerably weaker than the second, are observed at about 180 and 200 °C. The only explanation for this observation was that the peaks represented phase changes and/or melting of the decomposition product(s) of PPS. To verify whether this was true, DSC analyses were done on pure samples of different possible PPS decomposition products. Comparison of the two DSC curves in Figure 3.10 proves that $KHSO_4$ is, within reasonable doubt, the decomposition product of PPS when heated in a wax mixture. None of the other compounds gave DSC curves that looked nearly the same than the reheat curves discussed above. A possible explanation for this phenomenon is that the decomposing PPS extracts hydrogen from the wax chain and, in the process, functionalises the wax with sulphur and oxygen containing groups (see discussion under 3.4.3).

3.4.2 TG

The TG curves of the untreated wax and 10, 30 and 50% m/m mixtures of PPS with the wax are seen in Figure 3.11. Here the untreated wax shows only a small mass loss towards the end of the curve and gradually increasing mass losses, starting at approximately 150 °C, are observed for the mixtures containing increasing amounts of PPS.

3.4.3 FTIR

Figure 3.12 represents the FTIR spectra of the 10, 30 and 50% PPS mixed waxes. Table 3.4 is a summary of the bands appearing in these mixtures.

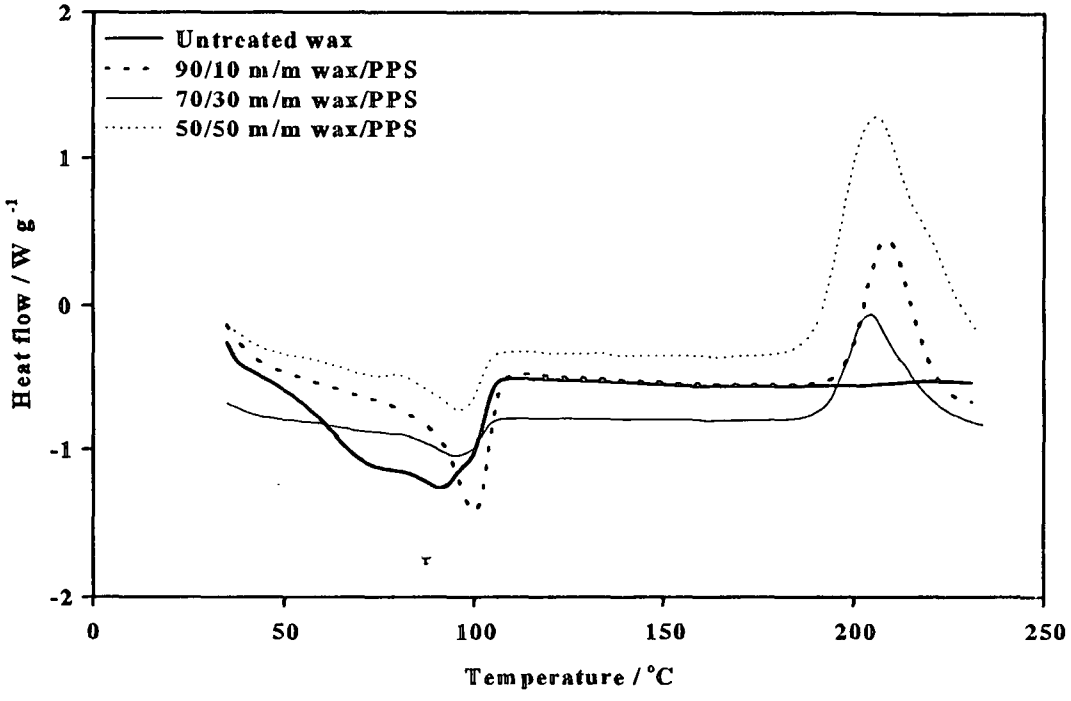

Figure 3.8 DSC curves of untreated wax 1 as well as samples mixed with different amounts of PPS

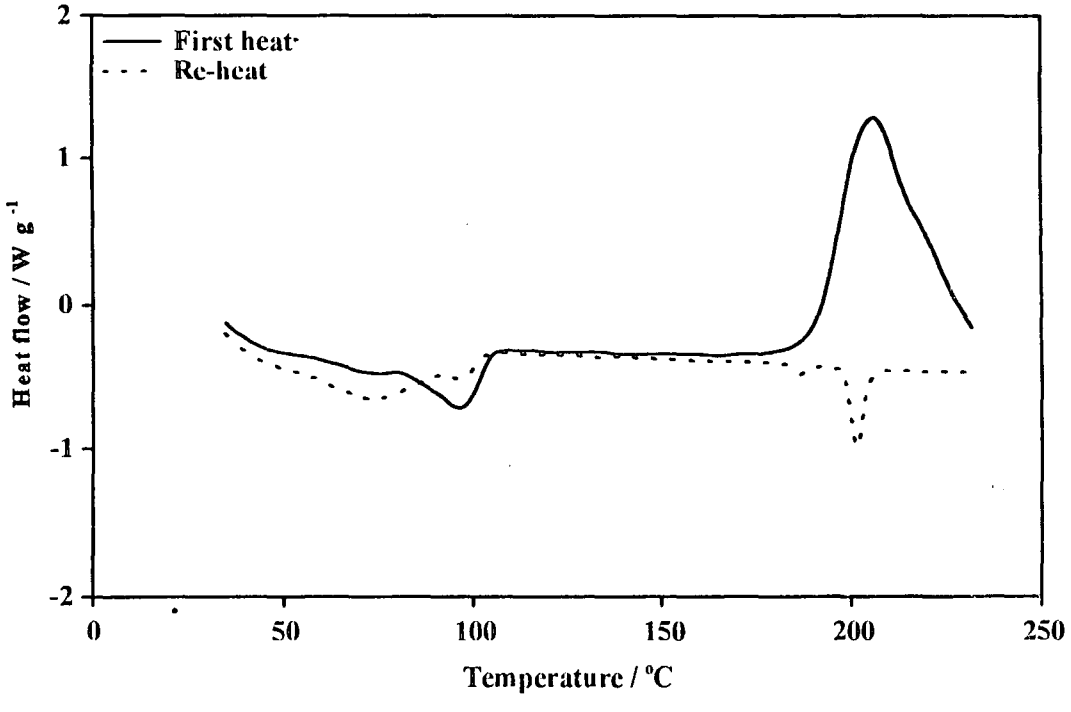

Figure 3.9 Heat and reheat curves of 50/50 m/m wax 1/PPS

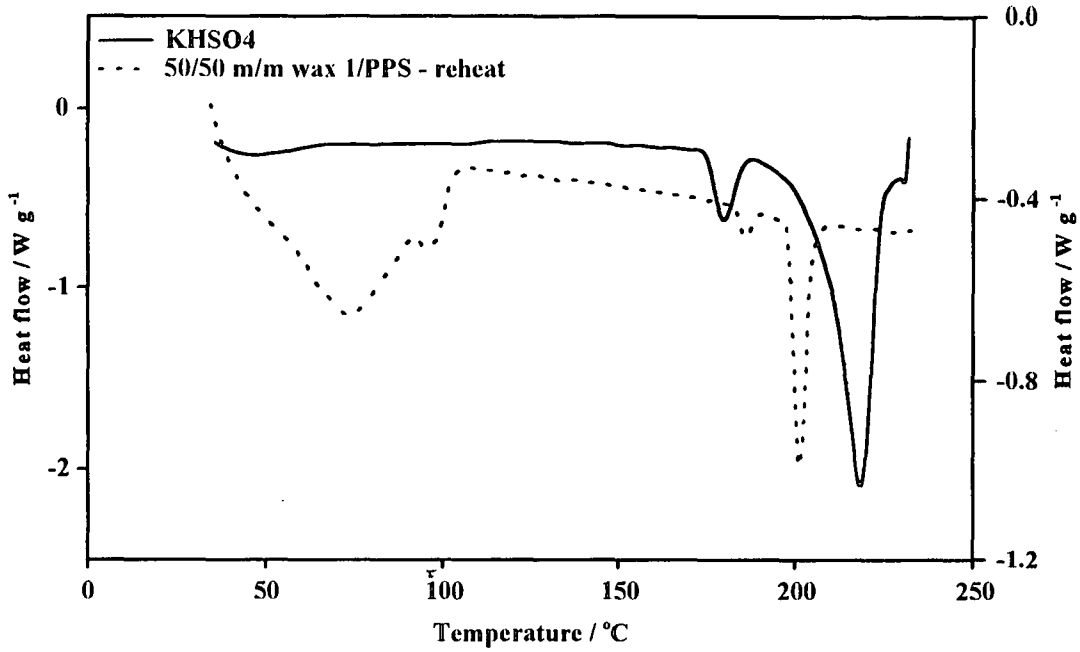

Figure 3.10 DSC curves for $KHSO_4$ and reheat of 50/50 m/m wax 1/PPS

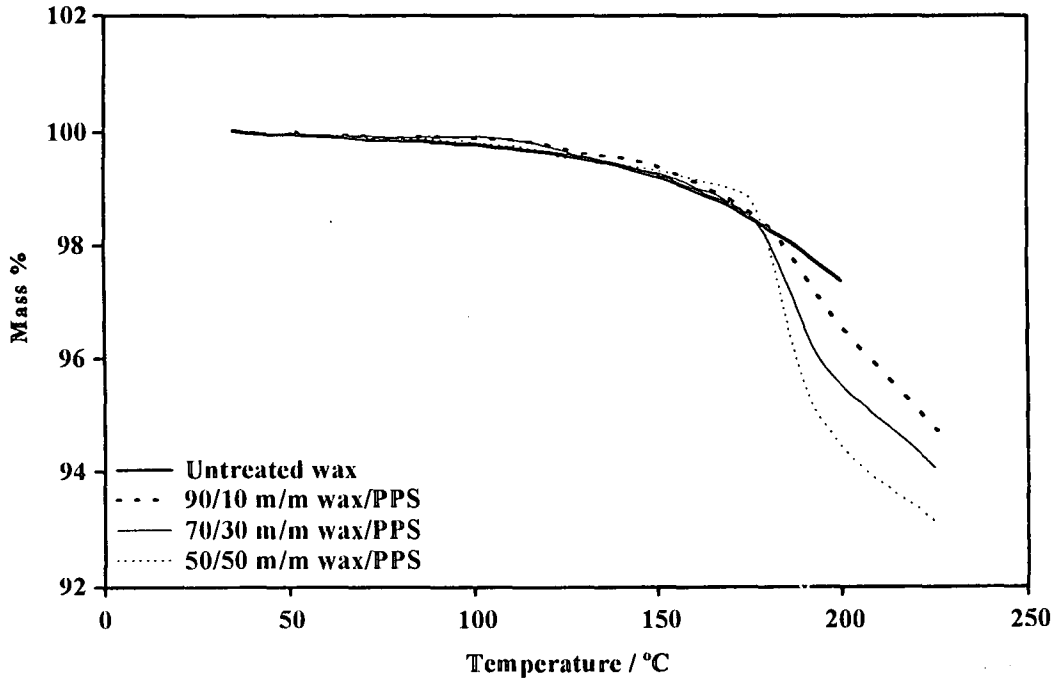

Figure 3.11 TG curves of untreated wax 1 as well as samples mixed with different amounts of PPS

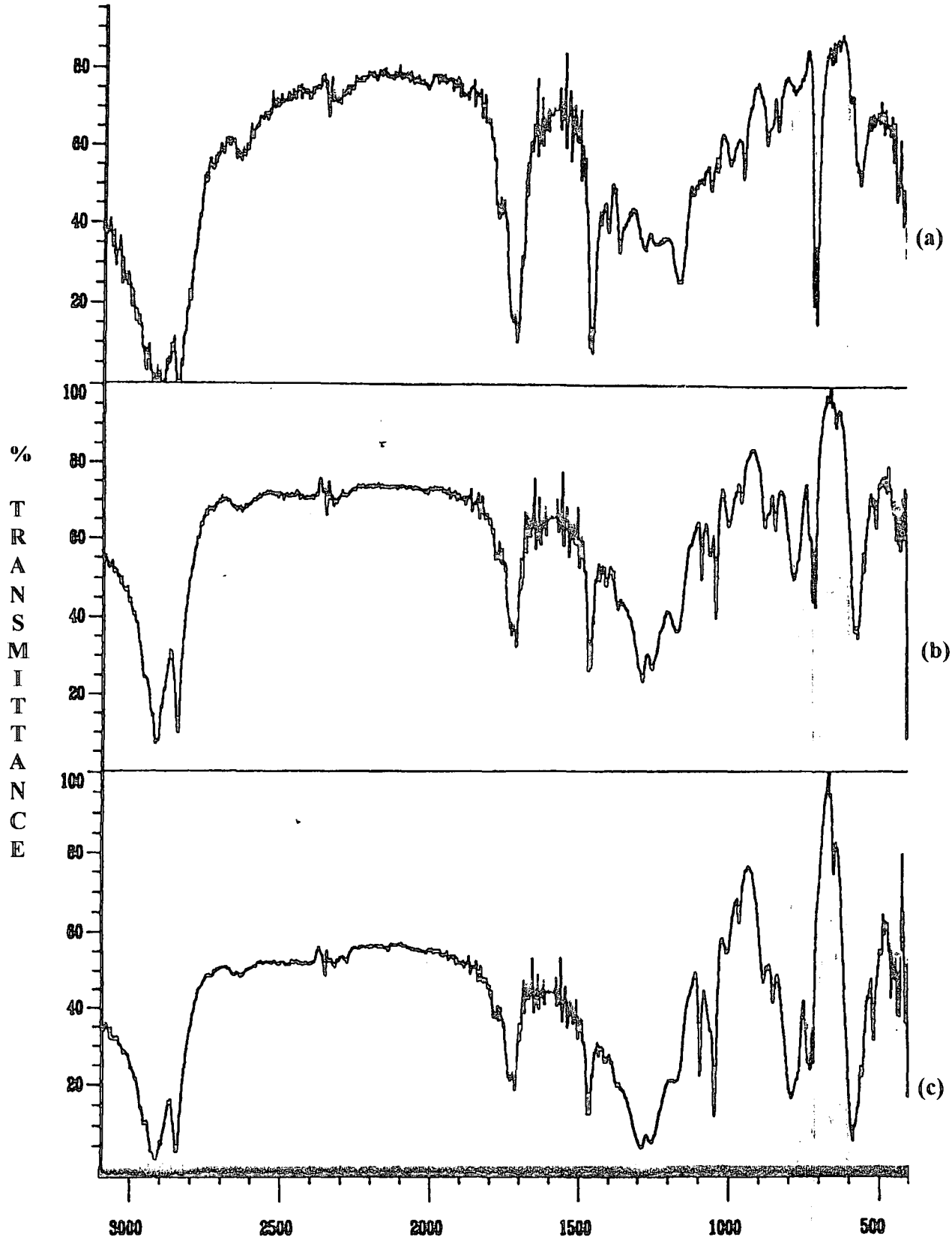

Figure 3.12 FTIR spectra of (a) wax 1 + 10 % PPS, (b) wax 1 + 30 % PPS, and (c) wax 1 + 50 % PPS

Table 3. 4 Summary of FTIR bands for PPS treated wax 1

90/10 m/m wax/PPS	70/30 m/m wax/PPS	50/50 m/m wax/PPS
2900-2850 cm^{-1} : C - H stretch (s)		
1710 cm^{-1} : C=O stretch (s)		
1475 cm^{-1} (s) CH_2 bending	1475 cm^{-1} (m) CH_2 bending	1475 cm^{-1} (w) CH_2 bending
1375 cm^{-1} : CH_3 bending		
1290 cm^{-1} (w) C-CO-C	1290 cm^{-1} (m) C-CO-C	1290 cm^{-1} (m) C-CO-C
1250-1050 cm^{-1} (w) S=O stretch	1250-1050 cm^{-1} (m) S=O stretch	1250-1050 cm^{-1} (m-s) S=O stretch
1020 cm^{-1} (w) S-O stretch		
950-720 cm^{-1} (w) out-of-plane bending (oop)		
~600 cm^{-1} (s) C-S		

(s) is strong intensity (m) is medium intensity (w) is weak intensity

The bands between 2900 to around 1500 cm^{-1} include the characteristic C-H stretching, C=O stretching in ketones, bending in the C-CO-C in ketones and CH_2 bending. Absorptions at 1375 cm^{-1} are normally characteristic of CH_3 bending, but here it may include any S=O stretching that may be present. The region 1250 to 1020 cm^{-1} shows characteristic bands for S=O and S-O stretching respectively. The intensities of these bands increase as the level of the initiator is increased. The bands between 950 and 720 cm^{-1} are indicative of long chains while strong absorption in the region from 720 to 620 cm^{-1} are indicative of C-S stretching in the case of mercaptans [35]. Therefore, there is a strong possibility that the band near 600 cm^{-1} is a C-S stretch. However, its slight shift to a lower frequency may be due to the presence of C-O bond. The C-S, S=O and S-O stretching absorptions may be indicative of functionalisation of the hydrocarbon chains in the presence of PPS.

3.5 Cross-linking of wax 2 in the presence of DCP

3.5.1 DSC

The DSC curves of the untreated wax and the 10, 30 and 50% m/m mixtures of DCP with the wax are shown in Figure 3.13. The untreated wax shows a double melting endotherm between 40 and 80 °C. Because DCP melts at only a slightly lower temperature than wax 2, the treated waxes show broad melting endotherms between 30 and 70°C, with the peak maxima shifting to lower temperatures as the amount of DCP increases. These endotherms are characteristic of an overlap between the melting events of substances with closely separated melting points. The decomposition/cross-linking exotherms between 150 and 200 °C are similar to what was observed for wax 1 and the explanation will be the same.

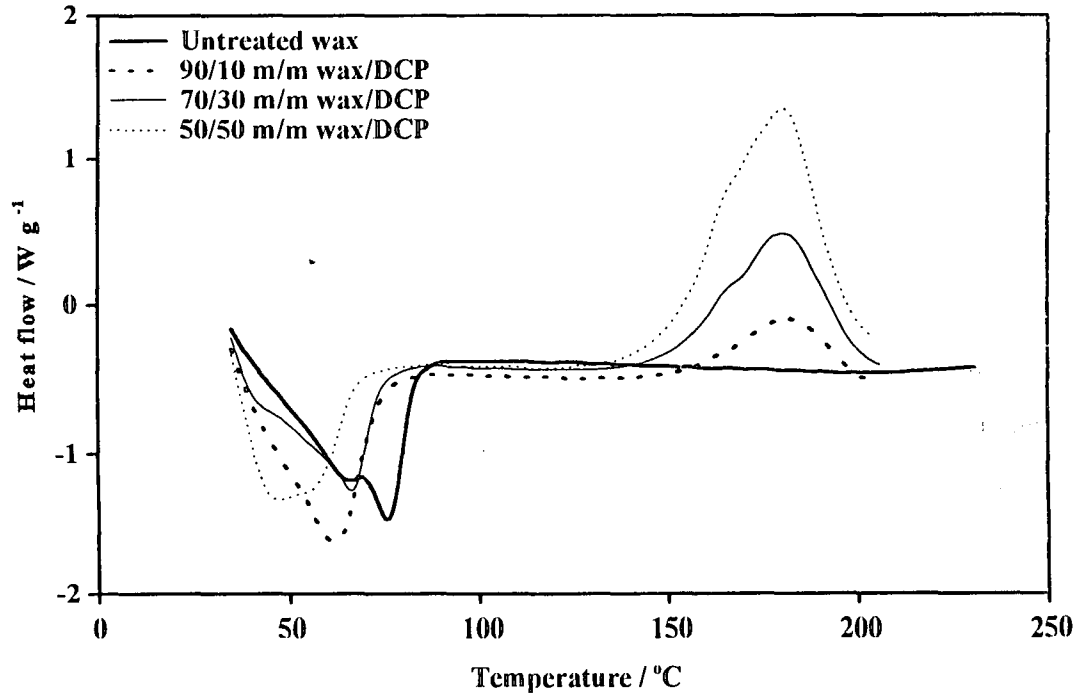

Figure 3.13 DSC curves of untreated wax 2 as well as samples mixed with different amounts of DCP

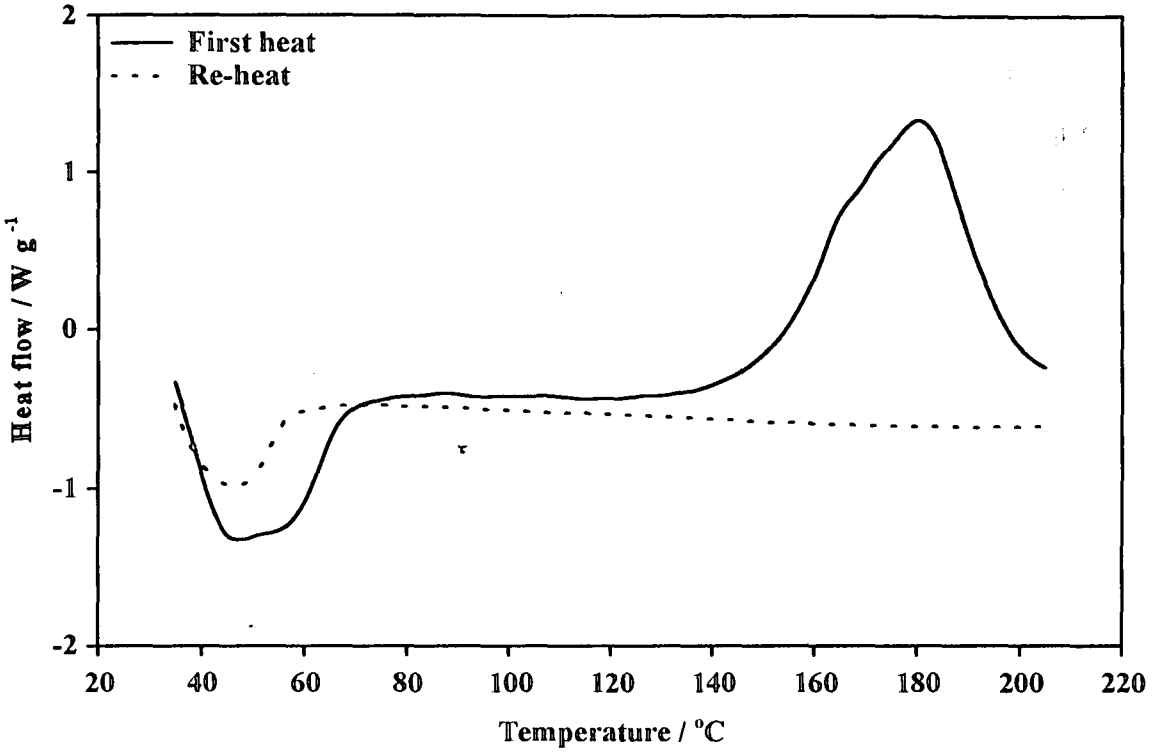

Figure 3.14 Heat and reheat curves of 50/50 m/m wax 2/DCP

As was the case with wax 1, the DSC reheat curves of the cross-linked samples (Fig. 3.14) show a smaller wax melting endotherm compared to the one observed during the first heating of the mixture. This is indicative of incomplete cross-linking of the wax.

3.5.2 TG

Thermogravimetric analysis results of the untreated and 10, 30 and 50% m/m DCP mixed waxes are shown in Figure 3.15. The TG curves show that the untreated wax has only a small mass loss of less than 5%, while the treated samples show mass losses of 9, 32 and 49% respectively, starting at about 160 °C. These values are in accordance with the amounts of DCP initially mixed into the wax.

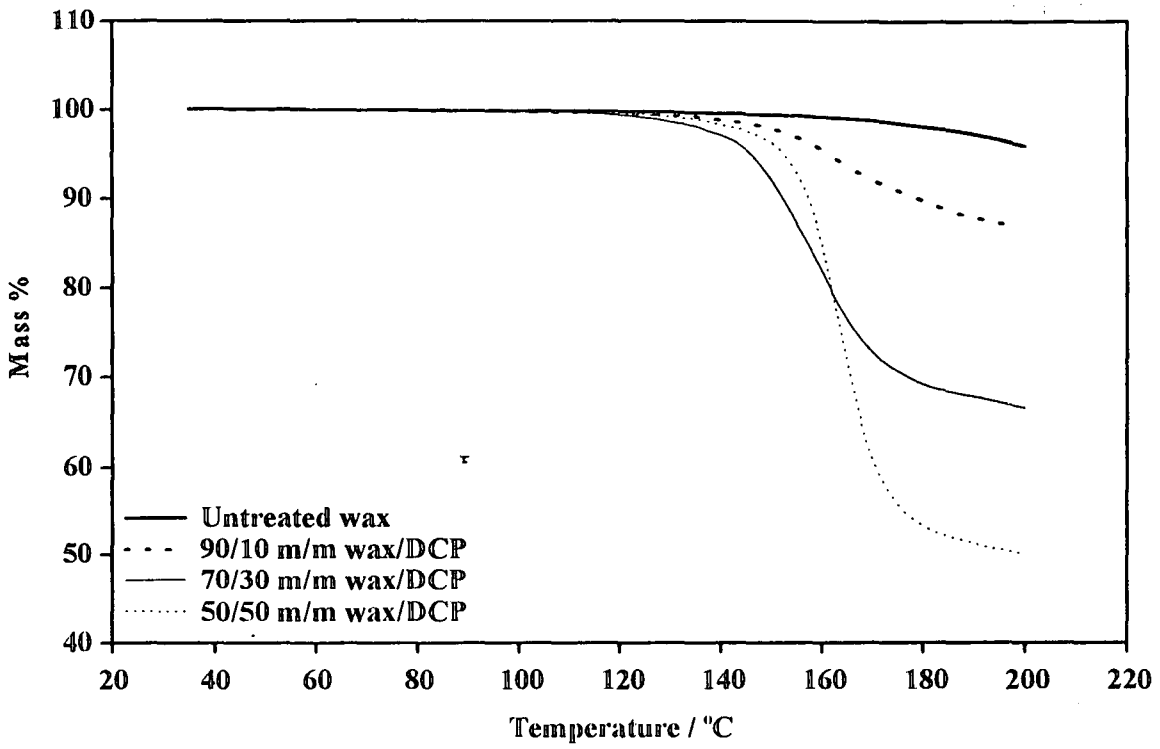

Figure 3.15 TG curves of untreated wax 2 as well as samples mixed with different amounts of DCP

3.5.3 FTIR

The FTIR spectrum of the untreated wax is shown in Figure 3.16 (a) and Figure 3.17 shows the spectra of the 10 and 30% mixed waxes. The 50% mixed wax is not seen as the cured mixture was too 'tacky' or 'sticky' and therefore could not mix with the potassium bromide in oder to form a spectral disc. A summary of the spectral bands for untreated, 10 and 30% mixed waxes is listed in Table 3.5.

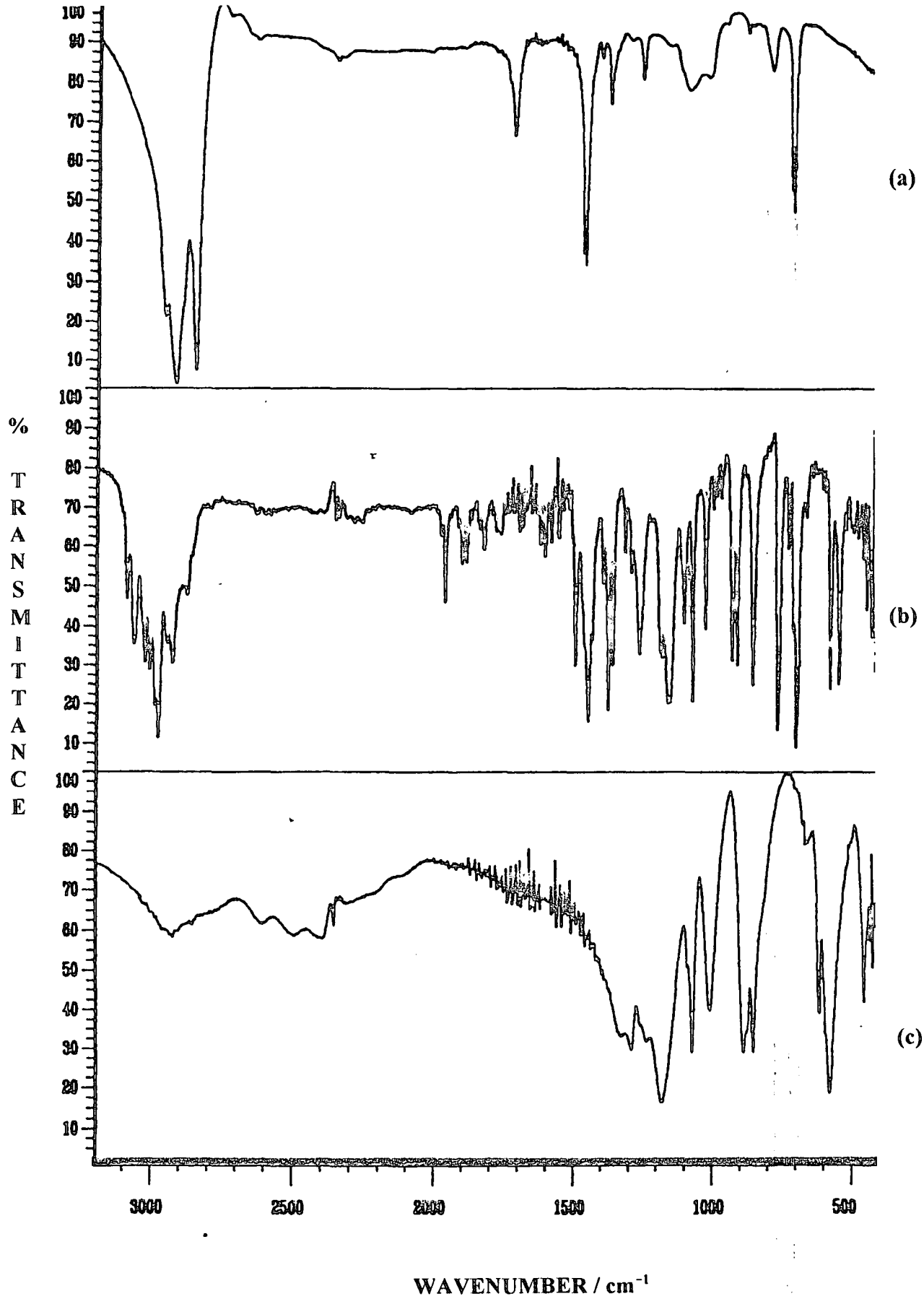

Figure 3.16 FTIR spectra of (a) untreated wax 2, (b) DCP, and (c) PPS

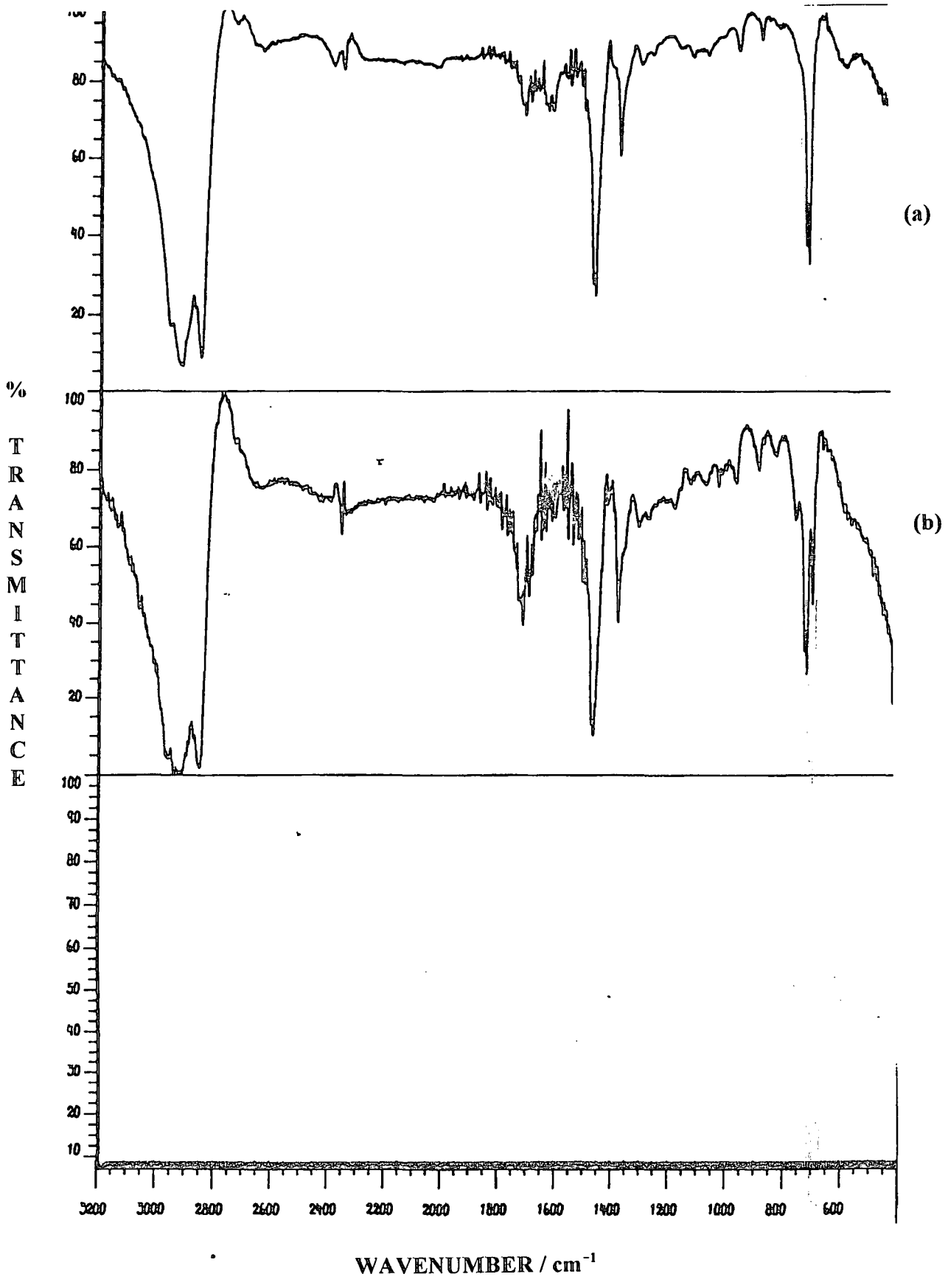

Figure 3.17 FTIR spectra of (a) wax 2 + 10 % DCP, and (b) wax 2 + 30 % DCP

Table 3. 5 Summary of FTIR bands for the untreated and treated wax 2

Untreated wax	90/10 m/m wax/DCP	70/30 m/m wax/DCP
2900-2800 cm^{-1} (s) C-H stretch	2900-2850 cm^{-1} (s) C-H stretch	2900-2800 cm^{-1} (s) C-H stretch
1710 cm^{-1} (m) C=O	1700 cm^{-1} (m) C=O	1700 cm^{-1} (m) C=O
	1600 cm^{-1} (m) C=C	1600 cm^{-1} (w) C=C
1475 cm^{-1} (s) CH_2 bending		
1375 cm^{-1} (m) CH_3 bending	1375 cm^{-1} (m) CH_3 bending	1375 cm^{-1} (s) CH_3 bending
1290-1000 cm^{-1} (m) C-O	1290 cm^{-1} (vw) C-O	
	950-900 cm^{-1} (w) C-O, =C-H out-of-plane bending (oop)	
720 cm^{-1} (s) long chain	725 cm^{-1} (s) long chain, out-of-plane bending	

(s) strong intensity (m) medium intensity (w) weak intensity (vw) very weak intensity

The absorption in the region 2900 to 2800 cm^{-1} is characteristic of C-H stretching. C=O bond is normally absorbed around 1700 cm^{-1} and it is possible that the C=O comes from ketones, carboxylic acids and esters. This absorption is noted to be of weak intensity in the 90/10 m/m wax/DCP sample and medium to strong intensity in the 70/30 m/m wax/DCP sample. The presence of acids and esters are confirmed by the C-O stretching between 1290 and 1000 cm^{-1}.

In alkenes, the C=C bond absorption is noted to occur between 1660 to1600 cm^{-1}. This band is absent in the untreated sample and decreases in the 70/30 m/m wax/DCP sample which indicates that the double bond is broken to form new bonds. The CH_2 and CH_3 bendings absorptions are seen at 1475 and 1375 cm^{-1} respectively. Furthermore, the intensity of the CH_3 bending absorption increases in the 70/30 m/m wax/DCP sample which again is in agreement with the diminishing C=C bond. The region 950 to 900 cm^{-1} is indicative of =C-H out-of-plane bending, but may include any overlapping C-O bond stretching that may be present. Finally, the band at 720 cm^{-1} confirms long chain structure [25].

3.6 Cross-linking of wax 2 in the presence of PPS

3.6.1 DSC

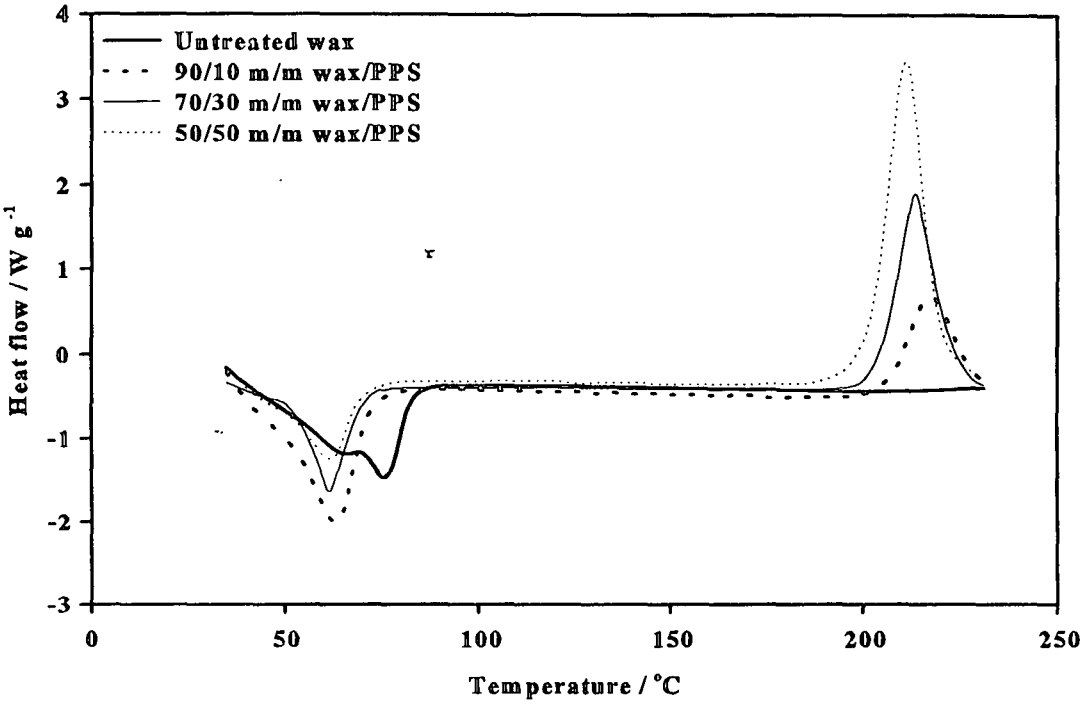

Figure 3.18 DSC curves of untreated wax 2 as well as samples mixed with different amounts of PPS

DSC thermal events of untreated and PPS treated wax 2 are seen in Figure 3.18. Untreated wax 2 melts in the temperature range 40 to 80 °C. The melting endotherms of the wax in the treated samples have different shapes to that of the untreated sample, indicating that the added PPS influenced the structure and melting behaviour of the wax. The peak intensities also decrease with increasing amount of PPS as a result of the smaller wax fractions in the respective samples. Exotherms, similar to the decomposition exotherm observed for pure PPS (Fig. 3.3), can be seen in the temperature range 200 to 230 °C. The increase in peak intensity relates to the increased PPS fractions in the samples. There is also a slight shift to lower temperatures with increased amount of PPS. Later I shall also show that, although cross-linking was initially thought to occur, the decomposition of PPS did not initiate cross-linking.

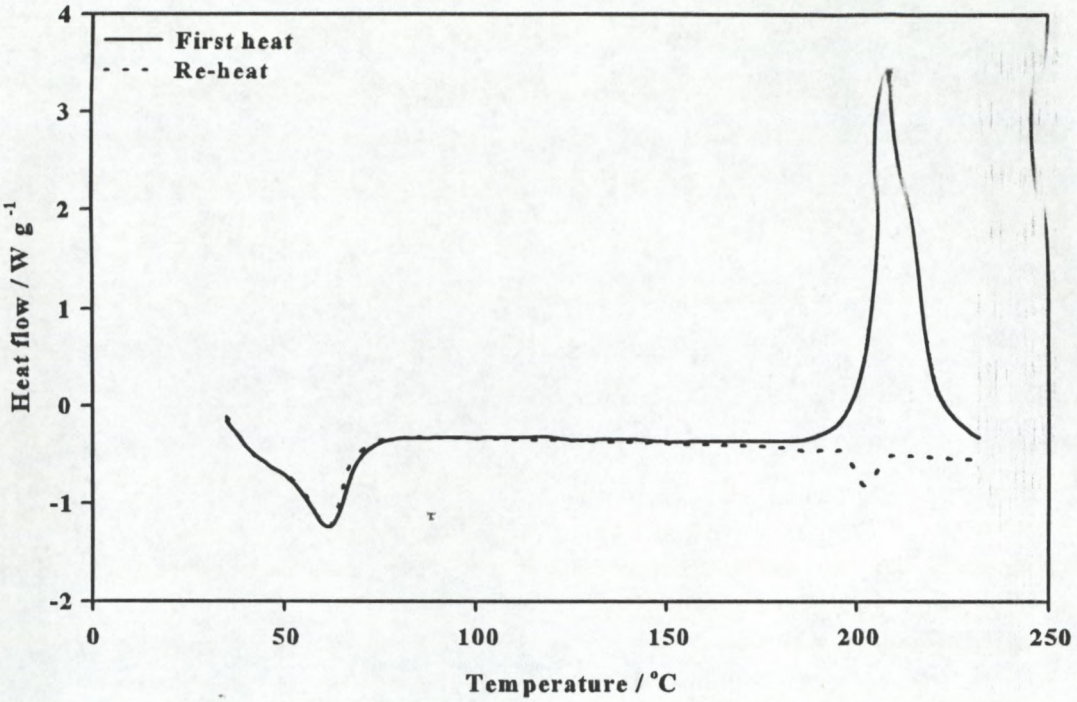

Figure 3.19 Heat and reheat curves of 50/50 m/m wax 2/PPS

Comparison of the heating and reheating DSC curves of a treated wax is shown in Figure 3.19. The melting endotherm of the wax in the sample did not change after heating it in the presence of PPS, indicating the absence of any cross-linking in this process. The two higher temperature endotherms in the reheat curve indicate, as discussed earlier, that PPS probably decomposed to $KHSO_4$, functionalising the wax in the process.

3.6.2 TG

Thermogravimetric analysis of treated and untreated samples of wax 2 can be seen in Figure 3.20. The untreated as well as treated samples show equivalent amounts of mass loss, indicating that the mass loss in this case is primarily due to wax degradation. Since we know that PPS decomposes to a certain extent, the small difference in total mass loss at 230 °C is probably due to evaporation of volatile PPS decomposition products.

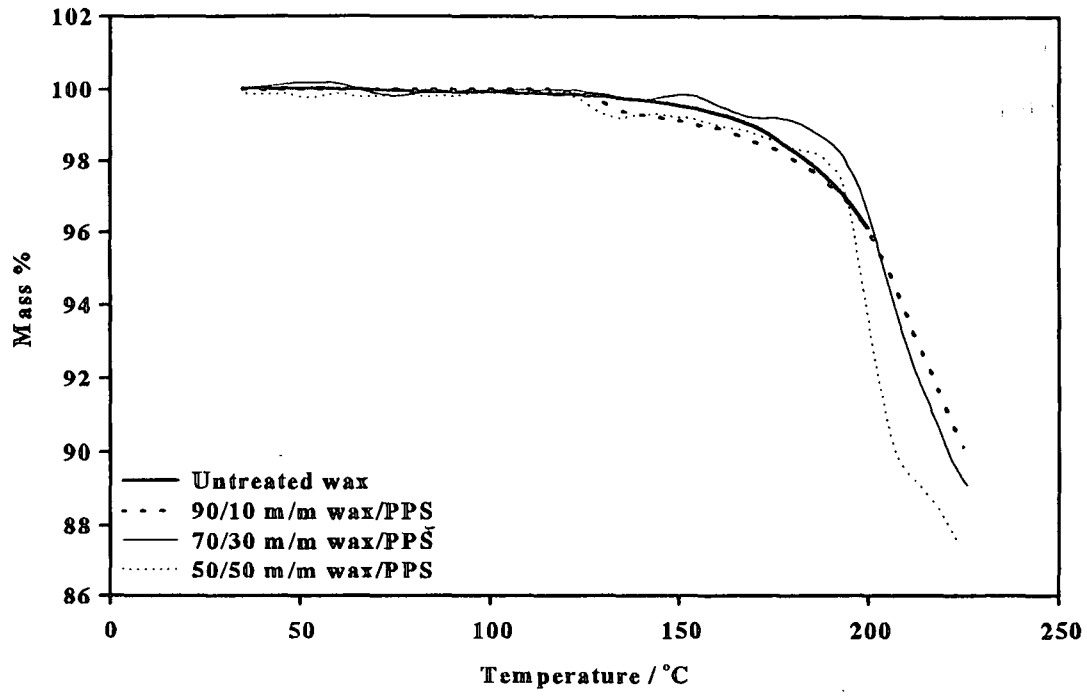

Figure 3.20 **TG curves of untreated wax 2 as well as samples mixed with different amounts of PPS**

3.6.3 FTIR

The FTIR spectra of the 10, 30 and 50 % PPS treated wax 2 is seen in Figure 3.21 (a), (b) and (c) respectively. A summary of the spectral absorptions is tabulated in Table 3.6.

Absorptions in the region 2975 to 2850 cm^{-1} can be assigned to the carbon-hydrogen stretching vibrations. CH_2 bending vibrations are accountable for the band at around 1460 cm^{-1} while CH_3 bending absorptions is characteristic near 1390 cm^{-1}. The C=O stretch near 1725 cm^{-1} is that of a normal aldehyde and this is confirmed by the band at 2750 cm^{-1}. Even though this band (-CHO) is weak in its intensity, it is very important as it is used to distinguish between ketones and aldehydes. However, its poor definition in the untreated wax may be due to the presence of other groups such as esters and ketones.

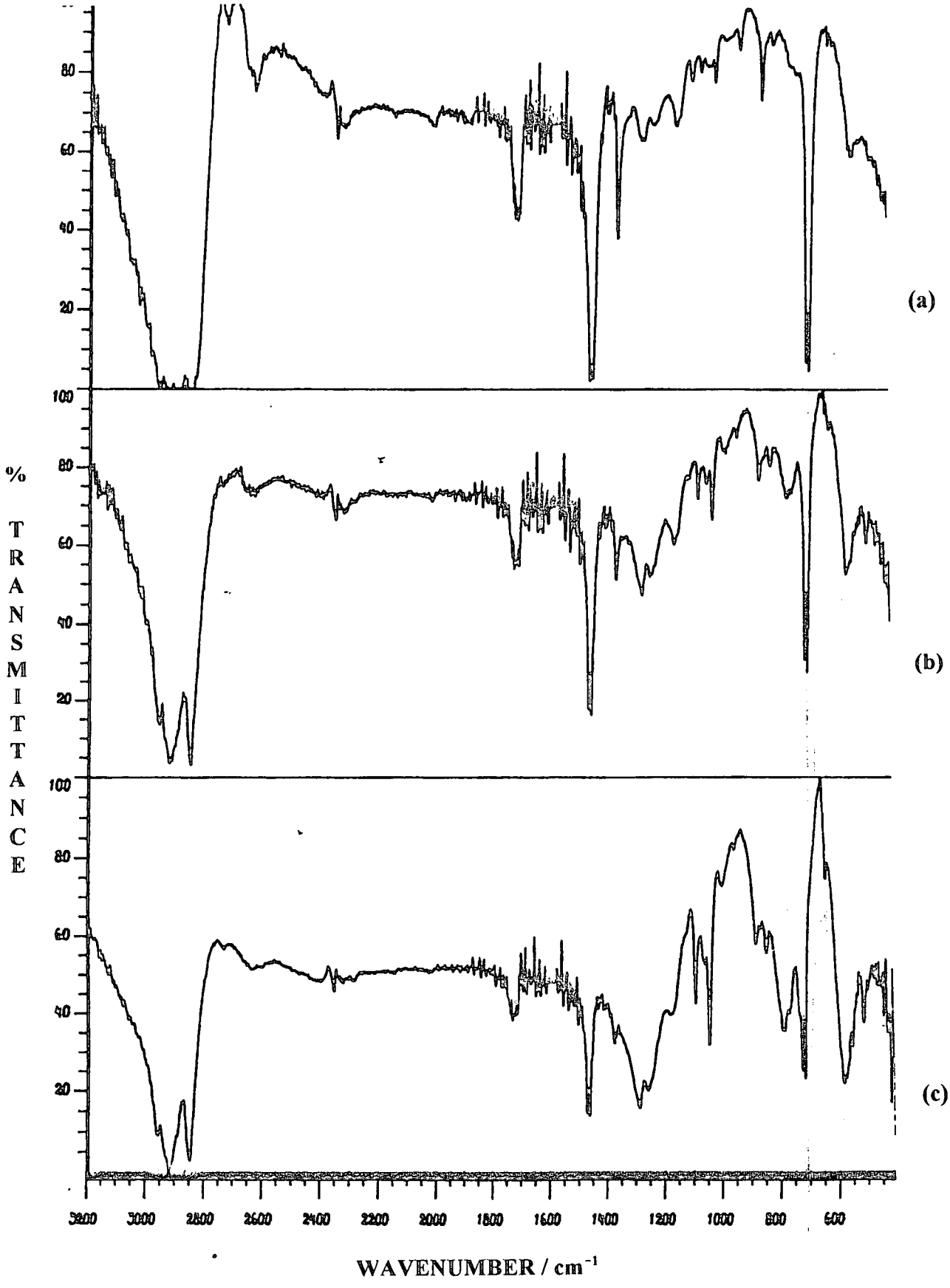

Figure 3.21 FTIR spectra of (a) wax 2 + 10 % PPS, (b) wax 2 + 30 % PPS, and (c) wax 2 + 50 % PPS

Table 3. 6 Summary of FTIR bands for the 10%, 30% and 50% PPS mixed waxes

Untreated wax 2	90/10 m/m wax/PPS	70/30 m/m wax/PPS	50/50 m/m wax/PPS
2975-2850 cm^{-1} : C-H stretch (s)			
	2750 cm^{-1} -CHO (w)	not clear	2750 cm^{-1} -CHO (vw)
	2650 cm^{-1} S-H (m)	2650 cm^{-1} S-H (w)	2650 cm^{-1} S-H (vw)
1725 cm^{-1} C=O (m)	1725 cm^{-1} C=O(s)	1725 cm^{-1} C=O (m*)	1725 cm^{-1} C=O (w*)
1475 cm^{-1} CH_2 bending(s)	1460 cm^{-1} CH_2 bending (s*)	1460 cm^{-1} CH_2 bending (m*)	1460 cm^{-1} CH_2 bending (w*)
1375 cm^{-1} CH_3 bending (m)	1380 cm^{-1} CH_3 bending, R-OSO_2-OR (s*)	1380 cm^{-1} CH_3 bending, R-OSO_2-OR (m*)	1380 cm^{-1} CH_3 bending, R-OSO_2-OR (w*)
1290 cm^{-1} C-O (m)	1300-1250 cm^{-1} C-O, C-SO_2-C (w✦)	1300-1250 cm^{-1} C-O, C-SO_2-C (m✦)	1300-1250 cm^{-1} C-O, C-SO_2-C (s✦)
	1175 cm^{-1} R-OSO_2-OR (w✦)	1175 cm^{-1} R-OSO_2-OR (m✦)	1175 cm^{-1} R-OSO_2-OR (s✦)
	1125 cm^{-1} C=O (w)		
1100-1000 cm^{-1} C-O (m)	1100-1000 cm^{-1} C-O, S=O (w✦)	1100-1000 cm^{-1} C-O, S=O (m✦)	1100-1000 cm^{-1} C-O, S=O (s✦)
	900 cm^{-1} S-O-C oop (s*)	900 cm^{-1} S-O-C oop (m*)	900 cm^{-1} S-O-C oop (w*)
750 cm^{-1} long chain band (s)	720 cm^{-1} long chain band (s*)	720 cm^{-1} long chain band (m*)	720 cm^{-1} long chain band (w*)
	600 cm^{-1} C-S (w✦)	600 cm^{-1} C-S (m✦)	600 cm^{-1} C-S (s✦)
		525 cm^{-1} C-S (m✦)	525 cm^{-1} C-S (s✦)

(s) - strong intensity (m)- medium intensity (w)- weak intensity (vw)- very weak intensity

(s*,m*,w*) - intensity relative to intensities in Figure 3.21(a)

(s✦, m✦, w✦) - intensity relative to intensities in Figure3.21 (c)

Although the S-H stretch is normally a weak band that occurs near 2560 cm $^{-1}$, it is possible that this group is accountable for the absorption around 2650 cm $^{-1}$. The slight shift to a higher frequency may be attributed to the C=O bond. It is observed that this band (S-H) is not present in the untreated wax but decreases in its intensity in the PPS mixed waxes as the PPS concentration is increased.

In addition to a C-O bond stretch, the S=O stretching band from sulphones also occurs in the 1300 to 1000 cm $^{-1}$ region. The increasing intensities of the band in this region of the PPS mixed waxes, indicates that the absorption due to the C-SO_2-C band is a strong possibility. Since the untreated wax 2 is free from sulphur containing compounds, it is safe to say that the band at 1290 cm $^{-1}$ is accountable to the C-O bond.

In the mixed waxes, there is a possibility that R-OSO_2-OR band occurs at 1175 cm^{-1} [35], but even if it is not this particular one, the band here is certainly due to a S=O stretching as the intensities are once again noted to increase as the PPS concentration is increased.

A well defined yet weak absorption band at 1125 cm $^{-1}$ in the 10% mixed wax, could be assigned to a C-O bond. However, this band is not present in the 30 and 50% mixed waxes, which may be due to the increased amount of the PPS.

In the region of 1100 to 1000 cm $^{-1}$, C-O bond stretching is characteristic in esters, ethers and carboxylic acids and it therefore may be typical for the untreated wax. On the other hand, the increase in intensity of this band with increasing concentrations of PPS shows that the band may be due to S=O band as this type of absorption also occurs here.

The range 1000 to 650 cm $^{-1}$ is used to analyse out-of-plane bending in alkenes as well as S-O bond stretching. In addition, C-S bond absorptions even though weakly exhibited, are also analysed in the region of 720 to 620 cm $^{-1}$ [35]. It is also noted that the bands at 900 cm $^{-1}$ appear to decrease in intensity with increased PPS concentration while the C-S band intensities in the 600 to 525 cm $^{-1}$ region increase with increasing PPS concentration.

Finally, the presence of long chain structure is confirmed by the band near 720 cm $^{-1}$ [25].

3.7 Cross-linking of wax 3 in the presence of DCP

3.7.1 DSC

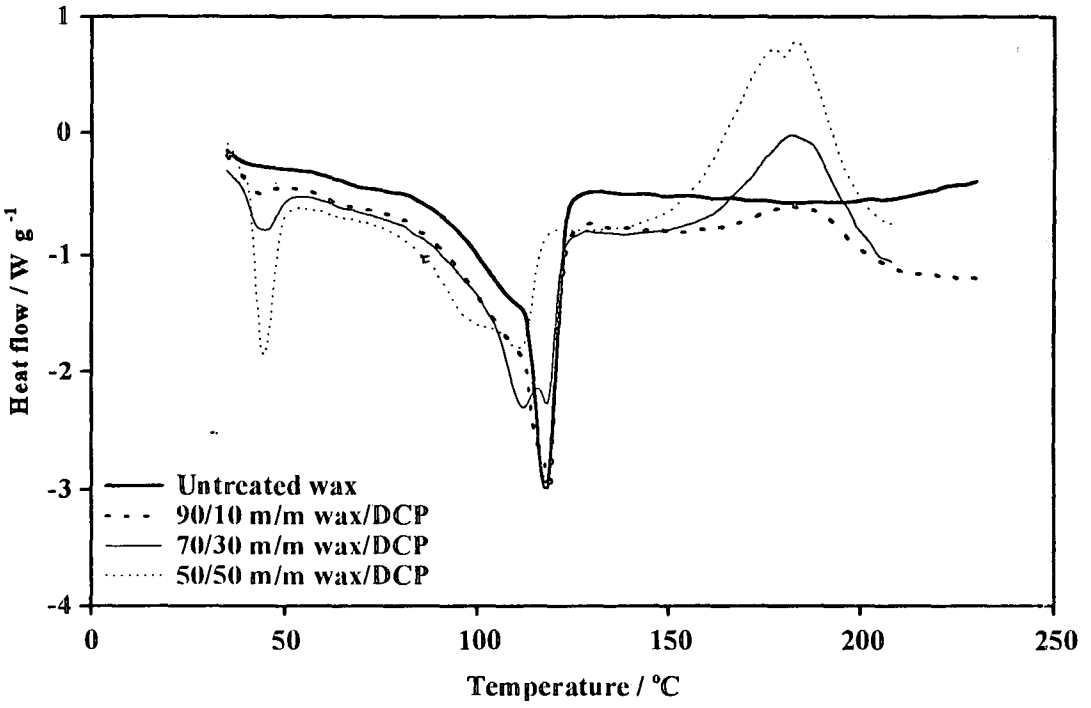

Figure 3.22 DSC curves of untreated wax 3 as well as samples mixed with different amounts of DCP

The melting endotherms of the wax in the different samples can be seen in the temperature range 90 to 120 °C. There are some differences in the shapes and sizes of these melting endotherms, indicating (i) the differences in amount of wax in the different samples and (ii) the influence of curing agent on the wax structure. The DCP melting endotherms appear in the temperature range 40 to 50 °C and the increased peak intensities are indicative of the increased fraction of DCP in the samples. As with the previous two waxes, broad strong exotherms are observed in the temperature range 150 to 200 °C, indicating decomposition of DCP and cross-linking of the wax. The sizes of the peaks are in line with the amounts of DCP mixed into the different wax samples. The 50/50 m/m wax/DCP sample clearly shows two peak maxima in this exotherm, which may be indicative of DCP decomposition immediately followed by wax cross-linking.

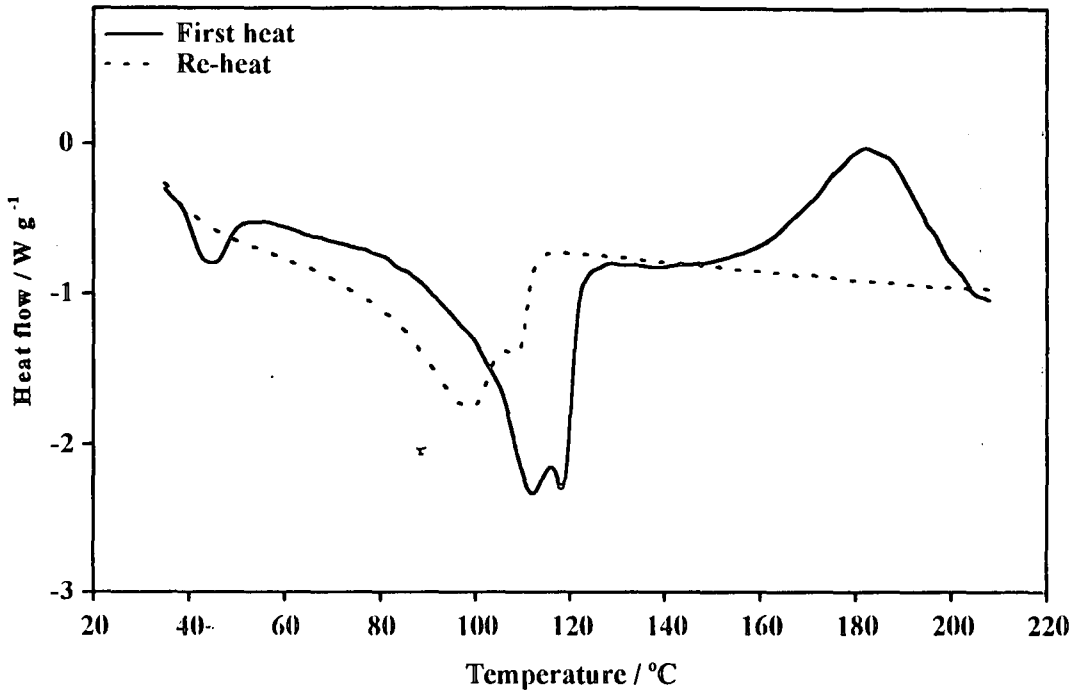

Figure 3.23 Heat and reheat curves of 70/30 m/m wax 3/DCP

In this case the reheating of the treated sample (Fig. 3.23) also serves as a proof that cross-linking did occur. The initial heat curve shows (i) the melting endotherm for DCP at about 40 °C, (ii) the wax melting endotherm between 100 and 120 °C, and (iii) the reaction exotherm between 150 and 200 °C. The reheat curve, however, only shows a wax melting endotherm which is clearly smaller than the initial melting endotherm and slightly shifted to a lower temperature. This indicates that a certain fraction of the wax must have been cross-linked.

3.7.2 TG

The TG analyses for this combination of wax and cross-linking agent do not differ much from what was observed and discussed for the previous two waxes (Fig. 3.24). Wax 3 only shows an extremely small mass loss over the temperature range, while the mass losses observed for the treated samples are in line with the values expected when all the DCP mixed into the samples decomposes and evaporates.

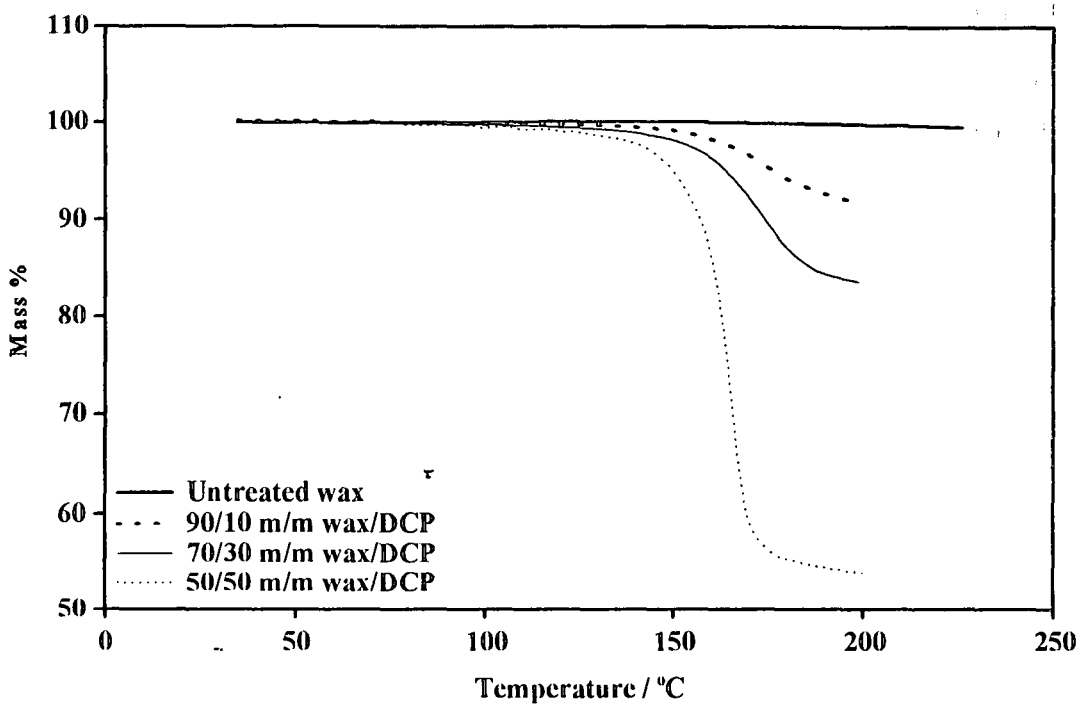

Figure 3.24 **TG curves of untreated wax 3 as well as samples mixed with different amounts of DCP**

3.7.3 FTIR

The FTIR spectra of the untreated and DCP mixed waxes are seen in Figure 3.25 (a) and Figure 3.26 (a), (b) and (c) respectively. A summary of the spectral absorptions is listed in Table 3.7.

Strong absorptions in the 2950 to 2850 cm^{-1} range, both in the untreated and the DCP mixed waxes, are due to C-H stretching. However the broadness of these bands indicate that the O-H stretching characteristic of carboxylic acids may be overlapped. Since this O-H is normally exhibited in the range of 3400 to2400 cm^{-1}, it is assumed that this stretch is also accountable for the bands between 2650 and 2400 cm^{-1} in the mixed waxes and between 2625 and 2375 cm^{-1} in the untreated wax.

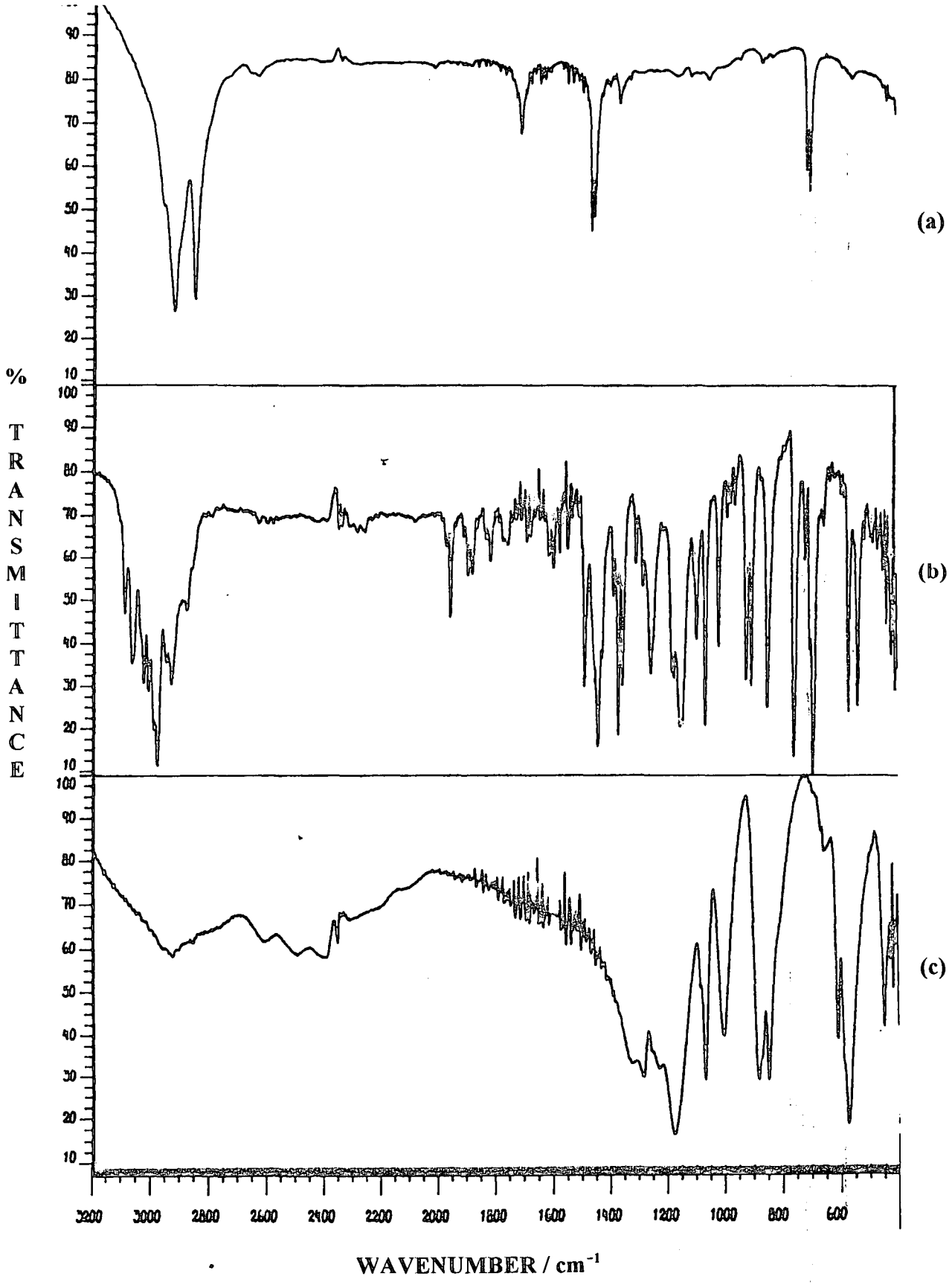

Figure 3.25 FTIR spectra of (a) untreated wax 3, (b) DCP, and (c) PPS

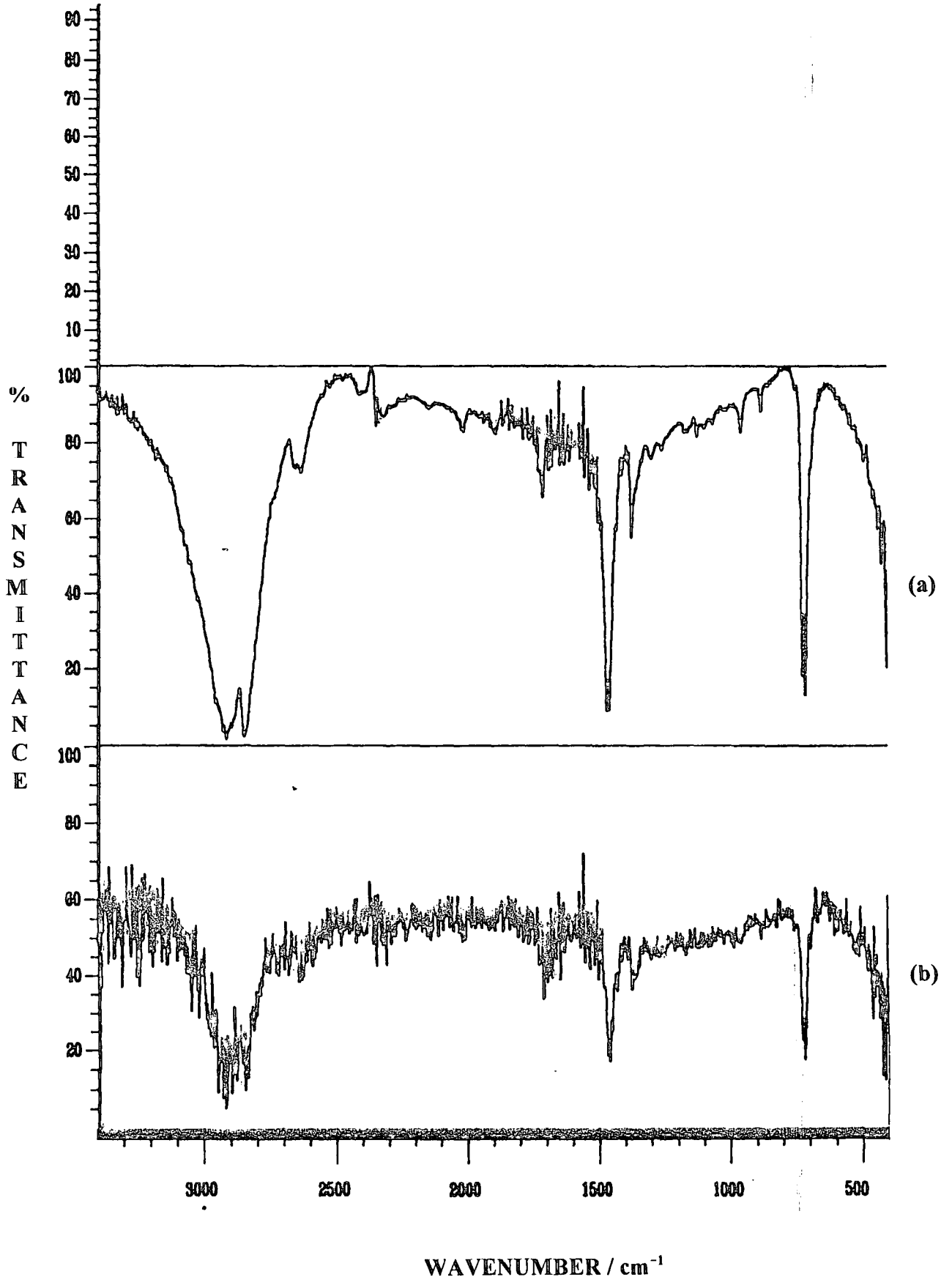

Figure 3.26 FTIR spectra of (a) wax 3 + 10 % DCP, and (b) wax 3 + 30 % DCP

Table 3.7 Summary of FTIR bands for the untreated and treated wax 3

Untreated	90/10 m/m wax/DCP	70/30 m/m wax/DCP
2975-2850 cm^{-1} (s) C-H stretch	2950-2850 cm^{-1} (s) C-H stretch	
2625-2375 cm^{-1} (w) O-H in carboxylic acids	2650-2400 cm^{-1} (m) O-H in carboxylic acids	
1725 cm^{-1} (s) C=O	1710 cm^{-1} (s) C=O	
1475 cm^{-1} (s) : CH_2 bending		
1375 cm^{-1} (m-w) CH_3 bending	1375 cm^{-1} (m) CH_3 bending	
1175-1075 cm^{-1} (w) C-O	1300-1075 cm^{-1} (w) C-O	
	950 cm^{-1} (w) O-H out-of-plane bending	
720 cm^{-1} (s) long-chain band		

(w) weak intensity (m) medium intensity (s) strong intensity

The bands seen at 1725 cm^{-1} in the untreated wax and at 1710 cm^{-1} in the mixed wax, are indicative of the carbonyl stretching vibration characteristics of aldehydes, ketones, carboxylic acids and esters. Methylene (CH_2) and methyl (CH_3) groups have characteristic bending absorptions in the regions near 1475 and 1375 cm^{-1} respectively.

The range of C-O bond absorptions that are present in ketones, carboxylic acids, ethers, alcohols and esters are normally seen between 1300 and 1000 cm^{-1} and therefore account for the bands appearing in this region of both the untreated and the mixed waxes. The absorption bands appearing at 950 cm^{-1} only in the spectra of the DCP mixed waxes are due to the hydrogen-bonded O-H out-of-plane bending vibrations which usually occur as low to medium intensity bands. Finally, the presence of long chains are confirmed by the strong band appearing near 720 cm^{-1} [25].

3.8 Cross-linking of wax 3 in the presence of PPS

3.8.1 DSC

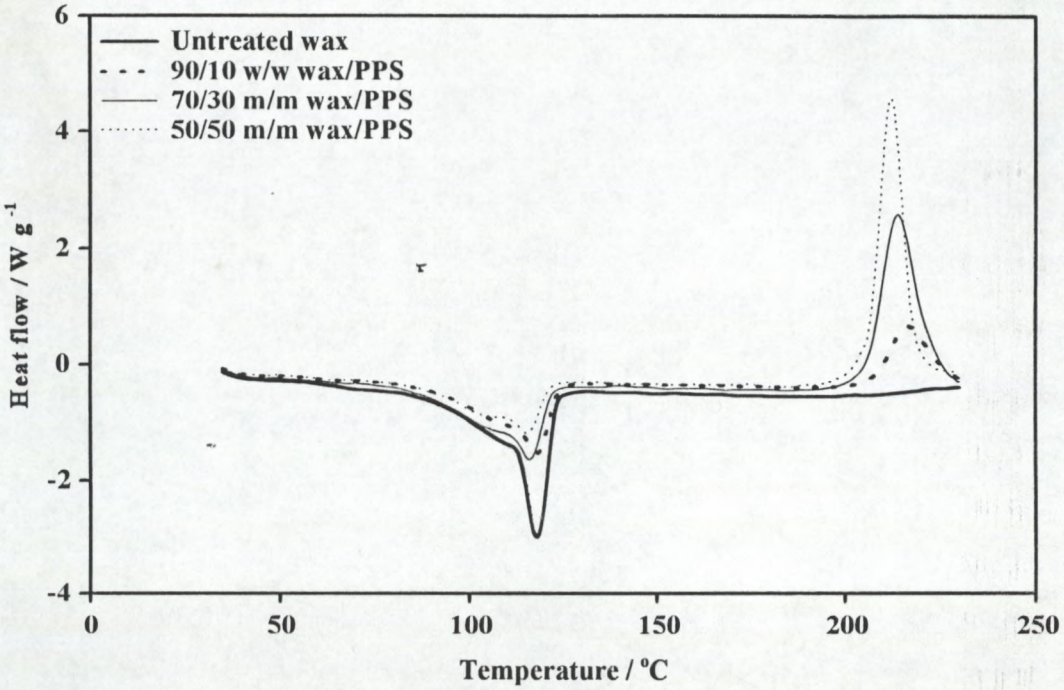

Figure 3.27 DSC curves of untreated wax 3 as well as samples mixed with different amounts of PPS

The DSC curves in Figure 3.27 show wax melting endotherms between 95 and 125 °C for all the samples. Contrary to the DSC analyses previously discussed, the melting peaks for the untreated and PPS treated samples have a similar shape, indicating that the history built into the initial wax structure was not disturbed by the presence of PPS. The respective peak sizes are also related to the fraction of wax present in each sample. The exotherms between 200 and 230 °C for the treated samples are for the decomposition of PPS and their respective heights are directly proportional to the amount of PPS initially mixed into the sample. As in the case of wax 2, these exotherms also shift to a slightly lower temperature with increasing PPS : wax ratio.

Comparison of the reheat curve with the initial heat curve (Fig. 3.28) shows essentially no decrease in size for the wax melting endotherms on reheating the samples. There is, however, a slight change in the shape and position of this endotherm compared to the endotherm during first heat. This again points to an absence of any cross-linking reaction in the presence of PPS, but functionalisation of the wax probably caused the change in shape and position of the wax melting endotherm. As was the case with the previous two waxes, the reheat curve displays two weak endotherms between 180 and 210 °C, typical of the phase transition and melting endotherms for $KHSO_4$.

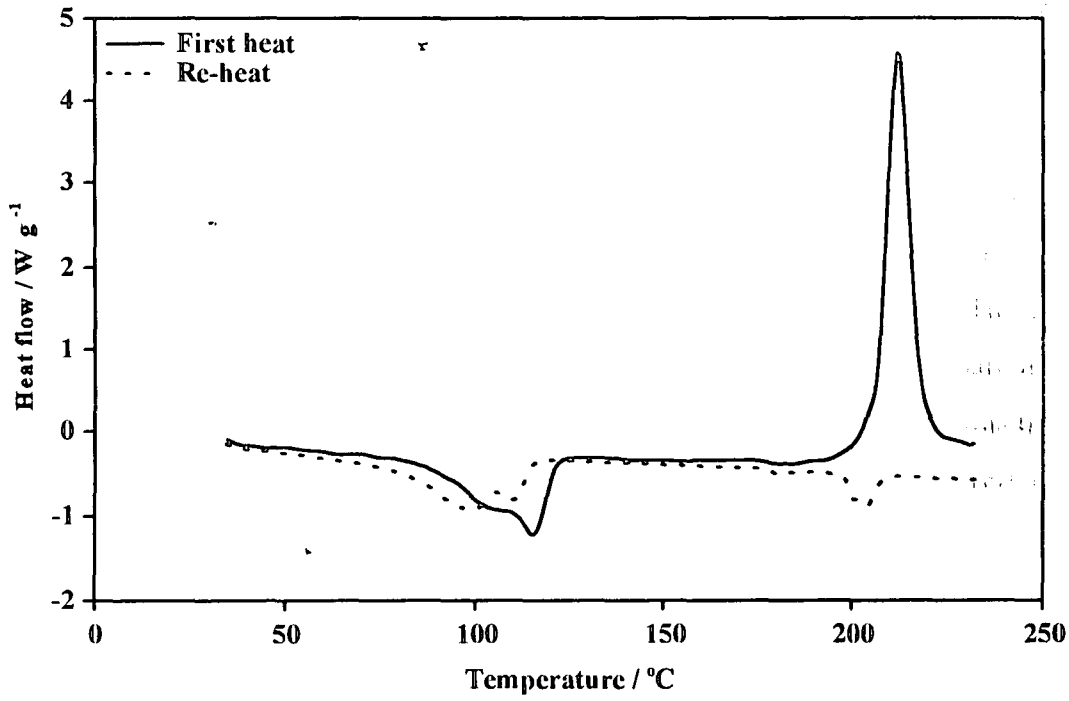

Figure 3.28 Heat and reheat curves of 50/50 m/m wax 3/PPS

3.8.2 TG

The TG curves (Fig. 3.29) follow essentially the same pattern observed for the previous waxes. The untreated wax shows an initial slight increase in mass, which may be attributed to moisture absorption. It did, however, show no significant mass loss up to the maximum temperature of analysis. The treated samples show small mass losses, starting at about 200 °C. The extent of mass loss for the respective samples is in relation to the initial amount of PPS mixed into each wax.

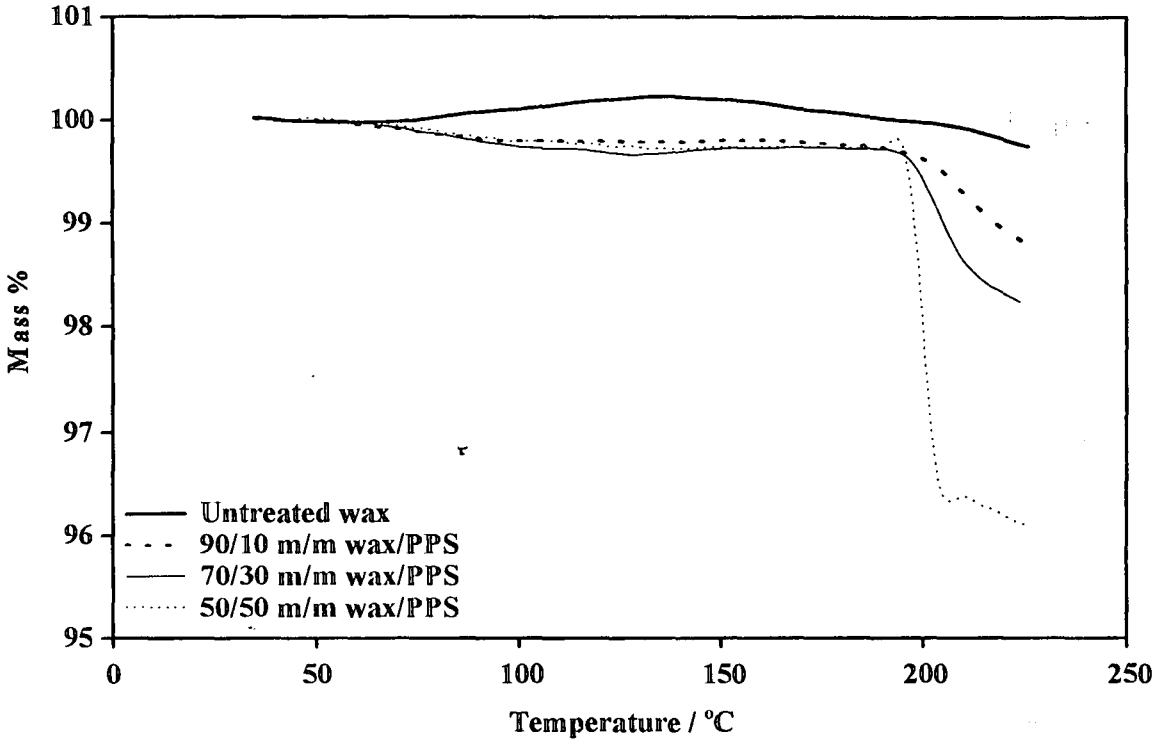

Figure 3.29 **TG curves of untreated wax 3 as well as samples mixed with different amounts of PPS**

3.8.3 FTIR

The spectrum of the untreated wax can be seen in Figure 3.25 (a) and that of the PPS mixed waxes are represented in Figure 3.30 (a), (b) and (c) respectively. Table 3.8 shows a summary of these spectral bands.

The most characteristic feature illustrated in Figure 3.30 is the broad shape of the bands occurring in the region from 3400 to 2400 cm^{-1} that are normally brought about by O-H absorptions in carboxylic acids. Overlapping absorptions in the 2950 to 2750 cm^{-1} region are generally assigned to the C-H stretching vibrations. These absorptions include sp^3 C-H absorptions since they occur at frequencies less than 3000 cm^{-1}.

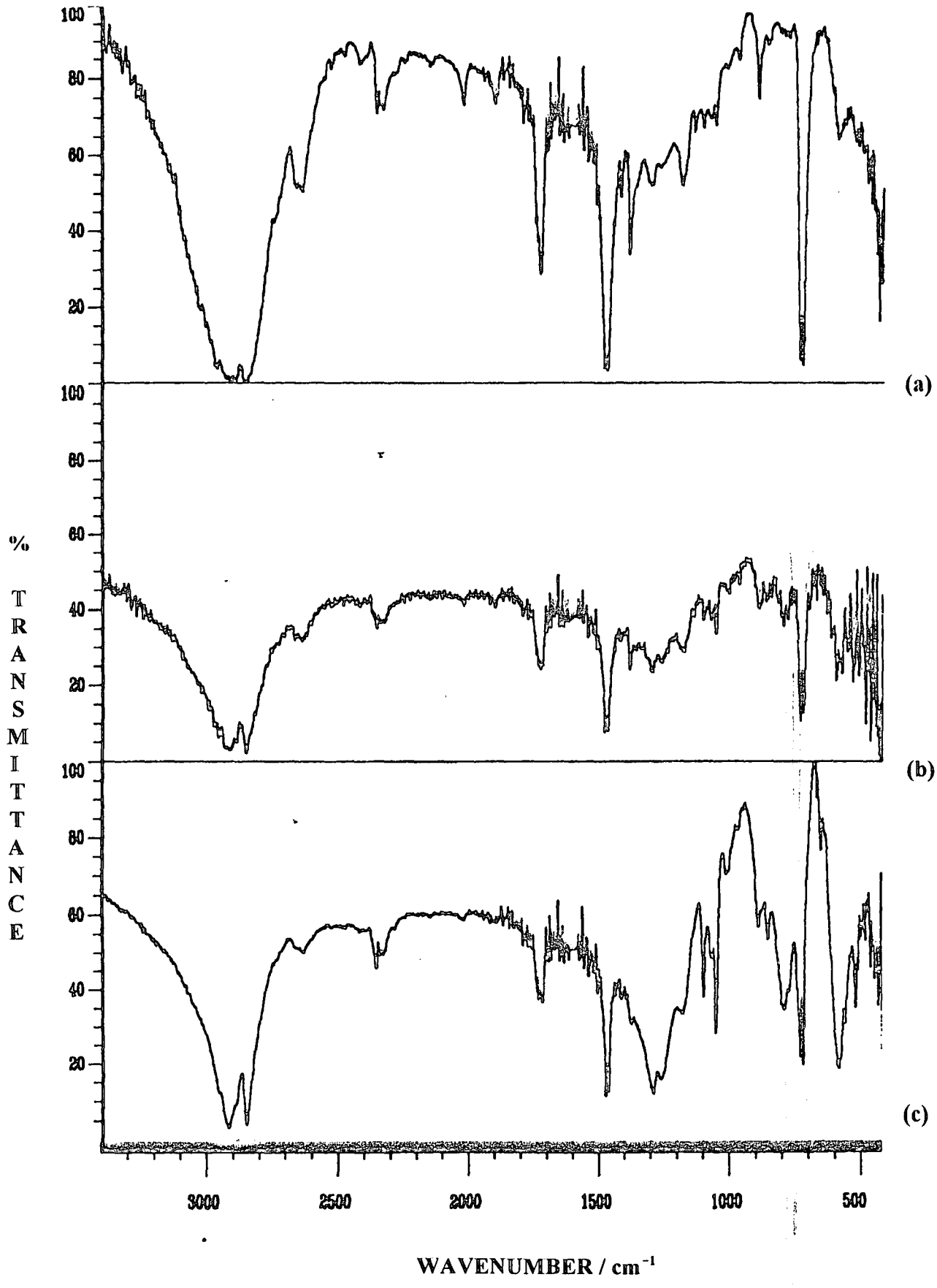

Figure 3.30 FTIR spectra of (a) wax 3 + 10 % PPS, (b) wax 3 + 30 % PPS, and (c) wax 3 + 50 % PPS

Table 3.8 Summary of FTIR bands for the untreated and treated wax 3

Untreated	90/10 m/m wax /PPS	70/30 m/m wax /PPS	50/50 m/m wax /PPS
2975-2850 cm $^{-1}$ (s) C-H stretch			
2625 cm $^{-1}$ (w) O-H, -CHO	2640 cm $^{-1}$ (m*) O-H, -CHO	2640 cm $^{-1}$ (m-w*) O-H, -CHO	
---	2410 cm $^{-1}$ (w) O-H	not clear	---
1725 cm $^{-1}$ (m) C=O	1710 cm $^{-1}$ (s) C=O		
1475 cm $^{-1}$ (s) CH_2 bending			
1375 cm $^{-1}$ (m-w) CH_3 bending	1375 cm $^{-1}$ (m) CH_3 bending		
950 cm $^{-1}$ (w) O-H out-of-plane bending			
------	800 cm $^{-1}$ (vw*) S-O	800 cm $^{-1}$ (w*) S-O	800 cm $^{-1}$ (s*) S-O
720 cm $^{-1}$ (s) long-chain band			
---	600 cm $^{-1}$ (m*) S-C		600 cm $^{-1}$ (s*) S-C

(s) strong (m) medium (w) weak (vw) very weak

(s*, m*, w*) intensity relative to Figure 3.30

The bands occurring at 2640 to 2625 cm $^{-1}$ may be attributed to the carboxylic O-H while the weak yet clearly defined absorption near 2410 cm $^{-1}$ that is present only in the 10% mixed wax may also be due to the O-H in carboxylic acids since it falls within this range. In aldehydes and ketones, the carbonyl stretching vibration (C=O) is normally between 1740 and 1705 cm $^{-1}$, while that of carboxylic acids occurs in the range of 1730 to 1700 cm $^{-1}$. Therefore the band at 1725 cm $^{-1}$ in the spectrum of the untreated will fall in the former and that in the spectra of the mixed waxes will fall in the latter.

Methylene ($-CH_2$) and methyl ($-CH_3$) bending in both the untreated and mixed waxes are evident at 1475 cm^{-1} and 1375 cm^{-1} respectively. The absorptions in the region between 1300 cm^{-1} and 1000 cm^{-1} account for the presence of the C-O stretch. In addition, it is assumed that S-H and S=O stretching that occurs only in the mixed waxes are overlapped here. It is also noted that the bands in the mixed waxes appear to increase in intensities from the 10 to 50% PPS, a trend similar to that of wax 1 and wax 2.

The band at 950 cm^{-1} can be attributed to the O-H out-of-plane bending vibration of carboxylic acids. This band naturally occurs as one of low to medium intensity as discussed in DCP mixed waxes. The S-O stretching vibrations are indicated by several strong bands in the region of 1000 cm^{-1} to 750 cm^{-1}. It can therefore be assumed that the bands appearing at 800 cm^{-1} in the mixed waxes are due to this stretch. Furthermore, it is also noted that the intensities of these bands increase as the amount of PPS is increased.

The presence of long chains in both the untreated and mixed waxes are again noted, as indicated by the absorption at 720 cm^{-1}. However, the region between 715 cm^{-1} and 620 cm^{-1} are indicative of S-C absorptions, although the mixed waxes show that these occur at 600 cm^{-1}. The shift to a lower frequency may be attributed to conjugation effects.

3.9 Gel content

3.9.1 Influence of DCP treatment on gel content of waxes

Table 3.9 Gel content values before and after treatment with different amounts of DCP

SAMPLE	% GEL CONTENT			
	UNTREATED WAX	WAX + 10 % DCP	WAX + 30 % DCP	WAX + 50 % DCP
Wax 1	6	10	33	70
Wax 2	11	13	30	48
Wax 3	1	23	37	67

The gel contents of the different samples were determined and the values are summarised in Table 3.10. For all three waxes there is a general increase in gel content with increasing amount of DCP mixed into the wax. There are small differences in the gel content values for untreated waxes and waxes cured in the presence of 10 % DCP. Higher DCP concentrations, however, give rise to increasingly higher gel content values indicating more effective cross-linking of the respective waxes. It is interesting to see that the maximum values for gel content increase in the order wax 1 > wax 3 > wax 2. According to the mechanism proposed by Brink and Dressler [12] the $PhC(CH_3)_2O\cdot$ and $CH_3\cdot$ free radicals, formed during the decomposition of DCP, attack the hydrocarbon chain removing hydrogen atoms. The unpaired electrons on two hydrocarbon free radical chains then combine to form a cross-link. We may reason that, in the case of an oxidised wax like wax 1, the hydrogen atoms in -OH groups are easier to remove than H-atoms in R-H, giving rise to a faster rate of cross-linking and eventually to a higher extent of cross-linking. Wax 3, which has a structure similar to that of wax 2, but with longer chains and a much narrower molar mass distribution, probably gives more efficient cross-linking because of more available sites per hydrocarbon chain.

3.9.2 Influence of PPS treatment on gel content of waxes

Table 3.10 Gel content values before and after treatment with different amounts of PPS

SAMPLE	% GEL CONTENT			
	UNTREATED WAX	WAX + 10 % PPS	WAX + 30 % PPS	WAX + 50 % PPS
Wax 1	4	6	6	6
Wax 2	12	12	14	14
Wax 3	1	1	3	3

The gel contents of the different samples were determined and the values are summarised in Table 3.10. For all three waxes the gel content values for untreated and treated samples were constant and within experimental error. This is a clear indication that no wax cross-linking occurred in the presence of potassium persulphate.

CHAPTER 4

CONCLUSIONS

All three of the investigated waxes cross-link in the presence of DCP and the decrease in size of the wax melting endotherms as well as the increase in wax gel content, which are measures of the extent of cross-linking, are proportional to the wax : DCP ratio. It further seems as if certain fractions of the waxes preferably cross-link, because there are changes in shape and temperature shifts of the wax melting endotherms compared to wax melting before cross-linking. It also seems as if the presence of DCP in the wax matrix has an influence on the structural history of the wax, giving rise to wax melting endotherms of different shapes depending on the amount of DCP mixed into the wax.

Wax 1 and 3 have much higher extents of cross-linking than wax 2, and it is believed that longer hydrocarbon chains and the presence of -OH groups favourably influence the rate of cross-linking of these waxes. In an extension of this study, the cross-linking kinetics of the different waxes can be investigated in order to verify whether this assumption is true.

The structures of all three waxes are changed when heated in the presence of DCP. This can be clearly seen in the C-H, CH_2 and CH_3 stretching regions in the FTIR analyses. The C-H stretchings are normally strong in the 3000 to 2850 cm^{-1} region, therefore this band may not confirm cross-linking as any significant change is unlikely to be noted. The intensities of the CH_2 and CH_3 bands show significant changes as discussed in the previous chapter. This is a strong indication of network formation. However, the wax became soft and "spongy" after heating of the 50/50 m/m wax/DCP of both wax 2 and 3, which rendered difficulties in the preparation of KBr discs necessary for FTIR analyses for better evaluation. PAS-FTIR, as discussed in Chapter 2, is a useful tool for such drawbacks. Unfortunately, this technique was not available during the course of this investigation and therefore is recommended for further investigations.

PPS does not initiate wax cross-linking, but instead influences the thermal history of the wax and funtionalises its hydrocarbon chains. This is illustrated by the change in shape and position of the wax melting peak when in the presence of PPS, and in the FTIR analyses of the PPS treated waxes, where S=O and S-O bond absorptions are clearly seen when the spectral regions of the untreated and PPS treated waxes are compared to that of PPS. There are further no conclusive spectroscopic evidence of wax cross-linking in the presence of PPS. Also, when PPS was mixed with the wax, $KHSO_4$ was identified as the solid decomposition product, instead of K_2SO_4 which is the decomposition product when PPS is heated on its own. This funtionalization is confirmed by the gel content as the results for the treated waxes show very little difference from that of the untreated wax contrary to that observed for the DCP mixed waxes.

As already mentioned, recommendations suggested are kinetic studies by thermal analysis, PAS-FTIR and comparison of the extent of degradation for cross-linked and uncross-linked waxes. In addition, computational molecular modeling [37] is recommended for those samples whose structures are known. This will enable simulation of the required reactions thus minimizing drawbacks that can occur in the experimental investigations.

REFERENCES

1. Hall, C, *Polymer Materials : An Introduction for Technologists and Scientists*, 1st edition, MacMillian Publishers, Hong Kong, 1981.
2. Holum, J R, *Fundamentals of General, Organic and Biological Chemistry*, 5th edition, Wiley and Sons, USA.
3. Gerans, G C, and Corbett, H R, *Spectrum* 28_3, August, 1990.
4. Hamilton, R Z, *Waxes : Chemistry, Molecular Biology and Functions*, 1st edition, The Oily Press, Dundee, 1995.
5. *Hawley's Condensed Chemical Dictionary*, 11th edition, pp 323.
6. Billmeyer, F W,Jr, *Textbook of Polymer Science*, 3rd edition, Wiley & Sons, USA, 1984.
7. *Comprehensive Polymer Science : The Synthesis, Characterization, Reactions and Applications of Polymers*, vol 6, Pergamon Press, Great Britain, 1989.
8. Naghash, H J, Okay, O, and Yagci, Y, *Polymer*, vol 38, No.5, pp 1187-1196, 1997.
9. Bellincampi, L D, and Dunn, M G, *Journal of Applied Science*, vol 63, 1997.
10. Mason, T J, *Sonochemistry : The uses of ultrasound in Chemistry*, The Royal Society of Chemistry, Cambridge, 1990.
11. Mason, T J, and Cordemans, E D, *Trans IChemE*, Vol 74, Part A July 1996.
12. Brink, A, and Dressler, F, *British Polymer Journal*, vol 1, 1969.
13. Jackson, P L, and Huglin, M B, *Eur. Poymer Journal*, vol 31, No. 31, pp 63-65, Great Britain, 1995.
14. Mallon, P E, McGill, W J, and Shillington, D P, *Journal of Applied Polymer Science*, vol 55, pp 705-721, 1995.
15. Pavlinec, J, and Lazar, M, *Journal of Applied Polymer Science*, vol 55, pp 39-45, 1995.
16. Wang, X M, Reidl, B, Christiansen, A W, and Geimer, *Polymer*, vol 35, No. 26, 1994.
17. Younes, M, Wartewig, S, Leillinger, D, Strehmel, B, and Strehmel, V, *Polymer*, vol 35, No. 24, 1994.
18. Hagen, R, Salmen, L, and Stenberg, B, *Journal of Polymer Science : Part B : Polymer Physics*, vol 34, pp 1997-2006, 1996.
19. Grobler, J H A, and McGill, W J, *Journal of Polymer Science : Part B : Polymer Physics*, vol 32, pp 287-295, 1994.
20. Martinez de la Granada, Sanz, J, and Martinez - Castro, I, *Journal of High Resolution Chromatography and Chromatography Communications*, Dr Alfred Heuthig Publishers, 1984.

21. Schromburg, G, Benecke, I, and Severin, G, *Journal of High Resolution Chromatography and Chromatography Communications*, Dr Alfred Heuthig Publishers, pp 391-394, 1985.

22. Benecke, I, and Schomburg, G, *Journal of High Resolution Chromatography and Chromatography Communications*, Dr Alfred Heuthig Publishers, pp 191-192, 1985.

23. Lui, H, Zhang, A, Jin, Y, and Fu, R, *Journal of High Resolution Chromatography*, vol 12, pp 537-539, August, 1989.

24. Hatakeyama, T, and Quinn, F X, *Thermal Analysis : Fundamentals and Applications to the Polymer Science*, Wiley & Sons Ltd, England, 1994.

25. Pavid, D L, *An Introduction to Spectroscopy*, 2nd edition, Saunders College Publishing, USA, 1996.

26. *Instrument operation manual*, MTEC Model 300.

27. *Sasolchem Technical Bulletin*, 1993.

28. Sienko, M J, and Plane, R A, *Chemistry*, 3rd edition, Kogakusha Co Ltd, Tokyo, 1996.

29. *Encyclopedia of Chemistry*, CSIR reference library.

30. Brown, M E, *Introduction to Thermal Analysis : Techniques and Applications*, Chapman & Hall, London, 1988.

31. *Annual Book of ASTM Standards*, pp 132-138, August, 1990.

32. Smith, B V, Waldron, N M, *Vogel's Elementary Practical Organic Chemistry Preparations*, 3rd edition, Longman, London.

33. Quintanilla, L, and Pastor, J M, *Polymer*, vol 35, No. 24, 1995

34. Haines, P J, *Thermal Methods of Analysis : Principles, Applications and Problems*, Chapman & Hall, UK, 1995.

35. *IR interpretation guide*, 410 Nicolet Impact Series.

36. *Compound Swell Test Procedure*, Dunlop BTR.

37. Caffery, M L, Dobosh, P A and Richardson, D A, *Laboratory Exercises Using HyperChem®*, Hypercube, Inc. Educational Publications, 1998.